Available online at www.sciencedirect.com
SCIENCE DIRECT®
ELSEVIER
International Journal of Solids and Structures 41 (2004) 6873–6894
INTERNATIONAL JOURNAL OF SOLIDS and STRUCTURES
www.elsevier.com/locate/ijsolstr

# Anti-symmetric waves in pre-stressed imperfectly bonded incompressible elastic layered composites

Sasikorn Leungvichcharoen, Anil C. Wijeyewickrema *, Taizo Yamamoto [1]

*Department of Civil Engineering, Tokyo Institute of Technology, O-okayama, Meguro-ku, Tokyo 152-8552, Japan*

Received 29 December 2003; received in revised form 18 May 2004
Available online 6 July 2004

**Abstract**

The effect of an imperfect interface on the dispersive behavior of in-plane time-harmonic symmetric waves in a pre-stressed incompressible symmetric layered composite, was analyzed recently by Leungvichcharoen and Wijeyewickrema (2003). In the present paper the corresponding case for time harmonic anti-symmetric waves is considered. The bi-material composite consists of incompressible isotropic elastic materials. The imperfect interface is simulated by a shear-spring type resistance model, which can also accommodate the extreme cases of perfectly bonded and fully slipping interfaces. The dispersion relation is obtained by formulating the incremental boundary-value problem and using the propagator matrix technique. The dispersion relations for anti-symmetric and symmetric waves differ from each other only through the elements of the propagator matrix associated with the inner layer. The behavior of the dispersion curves for anti-symmetric waves is for the most part similar to that of symmetric waves at the low and high wavenumber limits. At the low wavenumber limit, depending on the pre-stress for perfectly bonded and imperfect interface cases, a finite phase speed may exist only for the fundamental mode while other higher modes have an infinite phase speed. However, for a fully slipping interface in the low wavenumber region it may be possible for both the fundamental mode and the next lowest mode to have finite phase speeds. For the higher modes which have infinite phase speeds in the low wavenumber region an expression to determine the cut-off frequencies is obtained. At the high wavenumber limit, the phase speeds of the fundamental mode and the higher modes tend to the phase speeds of the surface wave or the interfacial wave or the limiting phase speed of the composite. The bifurcation equation obtained from the dispersion relation yields neutral curves that separate the stable and unstable regions associated with the fundamental mode or the next lowest mode. Numerical examples of dispersion curves are presented, where when the material has to be prescribed either Mooney–Rivlin material or Varga material is assumed. The effect of imperfect interfaces on anti-symmetric waves is clearly evident in the numerical results.


*Keywords:* Bifurcation; Dispersion; Elastic waves; Layered composite; Neutral curves; Pre-stress

* Corresponding author. Tel.: +81-357342595; fax: +81-357343578.
*E-mail address:* anil@cv.titech.ac.jp (A.C. Wijeyewickrema).
[1] Present address: Japan Highway Corporation, Kamihozumi 4-10-1, Ibaraki-shi, Osaka-fu 567-0036, Japan.

0020-7683/$ - see front matter © 2004 Elsevier Ltd. All rights reserved.
doi:10.1016/j.ijsolstr.2004.05.041

## 1. Introduction

The dispersive behavior of time harmonic in-plane symmetric waves in a pre-stressed incompressible symmetric layered composite with imperfect interface conditions, has been studied recently by Leungvichcharoen and Wijeyewickrema (2003), henceforth referred to as LW (2003). At the interface, stress increments and the displacement increment normal to the interface were assumed to be continuous, while the shear stress increment was assumed to be proportional to the jump in tangential displacement increments. The linear shear spring type resistance model employed to simulate the imperfect interface in LW (2003) can easily accommodate the extreme cases of perfectly bonded and fully slipping interfaces. In the present paper the corresponding case for time harmonic anti-symmetric waves is considered.

Previous work in the area of wave propagation in pre-stressed incompressible layers (Ogden and Roxburgh, 1993; Rogerson and Fu, 1995; Rogerson, 1997) and layered composites (Rogerson and Sandiford, 1996, 1997, 1999, 2000) are discussed in LW (2003) and will not be further elaborated on in this paper. Other recent related research is an extension of the work reported by Kaplunov et al. (1998) on asymptotically consistent theory for linear elastic thin-walled structures, to pre-stressed elastic layer problems, see for e.g. Kaplunov et al. (2000) for long-wave low-frequency motion, Pichugin and Rogerson (2001), Kaplunov and Rogerson (2002) and Nolde and Rogerson (2002) for long-wave high-frequency motion and Kaplunov et al. (2002) for short-wave high-frequency motion.

The basic equations of infinitesimal harmonic wave propagation in pre-stressed, incompressible, elastic media are given in Section 2. Using the propagator matrix, the dispersion relation for anti-symmetric motion is obtained in Section 3. It is shown that the dispersion relations for anti-symmetric and symmetric waves, differ from each other only through the elements of the propagator matrix associated with the inner layer. In Section 4 some interesting common features of these two kinds of waves viz. the asymptotic limits at low and high wavenumber limits are discussed. For the higher modes which have infinite phase speeds in the low wavenumber region, cut-off frequencies are investigated. Stability considerations not considered in LW (2003) are explored in detail for both anti-symmetric and symmetric waves in Section 5. Numerical examples using the same material parameters and pre-stressed conditions used in LW (2003), are presented in Section 6, where dispersion curves and neutral curves are plotted. In the case of dispersion curves the results for symmetric waves are only plotted for comparison as these curves were discussed in detail in LW (2003).

## 2. Basic equations

The equations for infinitesimal time-harmonic wave propagation in pre-stressed incompressible elastic media (see Dowaikh and Ogden, 1990; Rogerson and Sandiford, 1997; LW, 2003) are given in this section. Consider a homogeneous, incompressible, isotropic elastic body with an initial unstressed state $\mathfrak{B}_u$, which after being subjected to pure homogeneous strains has the new configuration $\mathfrak{B}_e$, the pre-stressed equilibrium state. A Cartesian co-ordinate system $Ox_1x_2x_3$, with axes coincident with the principal axes of strain is chosen for configuration $\mathfrak{B}_e$. Let $\mathbf{u}$ be a small, time dependent displacement superimposed on $\mathfrak{B}_e$. For the plane strain incremental problem considered here, the non-zero displacement components $u_i$, $(i = 1, 2)$ are independent of $x_3$. The incremental equations of motion where the linearized incompressibility condition $u_{i,i} = 0$ has been used is

$$\begin{aligned} &\mathscr{A}_{01111}u_{1,11} + (\mathscr{A}_{01122} + \mathscr{A}_{02112})u_{2,21} + \mathscr{A}_{02121}u_{1,22} - p_{,1} = \rho\ddot{u}_1, \\ &(\mathscr{A}_{01221} + \mathscr{A}_{02211})u_{1,12} + \mathscr{A}_{01212}u_{2,11} + \mathscr{A}_{02222}u_{2,22} - p_{,2} = \rho\ddot{u}_2, \end{aligned} \tag{1}$$

in which $\mathscr{A}_{0ijkl}$ are the components of the fourth-order tensor of first-order instantaneous moduli of incompressible isotropic elastic material which relates the nominal stress increment tensor and the deformation gradient increment tensor and can be given in terms of derivatives of the strain energy function (Ogden, 1984, p. 344), $p$ the incremental pressure, $\rho$ the material density and superimposed dot and comma indicate differentiation with respect to time $t$ and the spatial coordinate component in $\mathfrak{B}_e$, respectively.

The relevant components of the nominal stress increment tensor in the configuration $\mathfrak{B}_e$ are expressed as,

$$\begin{aligned} s_{021}(x_1,x_2,t) &= \mathscr{A}_{02121}u_{1,2} + (\mathscr{A}_{02112}+\bar{p})u_{2,1}, \\ s_{022}(x_1,x_2,t) &= \mathscr{A}_{02211}u_{1,1} + (\mathscr{A}_{02222}+\bar{p})u_{2,2} - p, \end{aligned} \tag{2}$$

where $\bar{p} = \mathscr{A}_{02121} - \mathscr{A}_{01221} - \sigma_2$ (Rogerson and Fu, 1995) is a quasi-static pressure in which $\sigma_2$ is the principal Cauchy stress in the $x_2$-direction in $\mathfrak{B}_e$.

The displacement and pressure increments for harmonic waves propagating in $x_1$-direction, may be expressed as

$$(u_1,u_2,p) = (A_1,A_2,kP)\mathrm{e}^{qkx_2}\mathrm{e}^{\mathrm{i}k(x_1-vt)}, \tag{3}$$

where $k$ is the wavenumber, $v$ the phase speed, $A_1$, $A_2$ and $P$ are unknown coefficients and the parameter $q$ is to be determined. Substituting Eq. (3) into Eq. (1) and using the linearized incompressibility condition, yields a system of homogeneous equations for which a non-trivial solution exists provided that

$$\gamma q^4 - (2\beta - \rho v^2)q^2 + (\alpha - \rho v^2) = 0, \tag{4}$$

where $\alpha = \mathscr{A}_{01212}$, $2\beta = \mathscr{A}_{01111} + \mathscr{A}_{02222} - 2\mathscr{A}_{01122} - 2\mathscr{A}_{01221}$ and $\gamma = \mathscr{A}_{02121}$ and the four roots of $q$ are given by $\pm q_m$ $(m = 1,2)$. From the definition of instantaneous elastic moduli of incompressible isotropic elastic material, the parameters $\alpha$, $\beta$ and $\gamma$ are expressed in terms of the strain energy function $W$ and the principal stretches $\lambda_1$ and $\lambda_2$ as (Dowaikh and Ogden, 1991),

$$\begin{aligned} &\alpha\lambda_2^2 = \gamma\lambda_1^2 = (\lambda_1 W_1 - \lambda_2 W_2)\lambda_1^2\lambda_2^2/(\lambda_1^2 - \lambda_2^2), \\ &2\beta + 2\gamma = \lambda_1^2 W_{11} + \lambda_2^2 W_{22} - 2\lambda_1\lambda_2 W_{12} + 2\lambda_2 W_2, \end{aligned} \tag{5}$$

where $W_i = \partial W/\partial\lambda_i$, $W_{ij} = \partial^2 W/\partial\lambda_i\partial\lambda_j$, $(i,j = 1,2)$ and when $\lambda_1 = \lambda_2 = \lambda$, Eq. (5) reduces to $\alpha = \beta = \gamma = \frac{1}{2}\lambda(\lambda W_{11} - \lambda W_{12} + W_1)$. In addition, the strong ellipticity conditions (Dowaikh and Ogden, 1990)

$$\alpha > 0, \qquad \gamma > 0, \qquad \beta > -\sqrt{\alpha\gamma}. \tag{6}$$

are necessary for stable in-plane harmonic wave propagation in the pre-stressed elastic material, and will be considered in Section 5 when the stability criteria of wave propagation in layered composites are discussed.

In order to obtain the propagator matrix, the incremental displacements and stresses in Eqs. (2) and (3) are written in the form of a $4\times1$ vector as

$$(u_1,u_2,s_{021},s_{022})^{\mathrm{T}} = [U_1(x_2),U_2(x_2),S_{021}(x_2),S_{022}(x_2)]^{\mathrm{T}}\mathrm{e}^{\mathrm{i}k(x_1-vt)}. \tag{7}$$

From Eq. (7) it can be shown after some manipulation that

$$\mathbf{y}(x_2) = \mathbf{H}\mathbf{E}(x_2)\mathbf{a}, \tag{8}$$

where $\mathbf{y}(x_2)$ is a displacement–stress increment vector and $\mathbf{E}(x_2)$ is a diagonal matrix given by

$$\begin{aligned} \mathbf{y}(x_2) &= \left[-\mathrm{i}U_1(x_2), U_2(x_2), \frac{S_{021}(x_2)}{\mathrm{i}k}, \frac{S_{022}(x_2)}{k}\right]^{\mathrm{T}}, \\ \mathbf{E}(x_2) &= \mathrm{diag}(\mathrm{e}^{q_1kx_2}, \mathrm{e}^{-q_1kx_2}, \mathrm{e}^{q_2kx_2}, \mathrm{e}^{-q_2kx_2}), \end{aligned} \tag{9}$$

and $\mathbf{a}$ is a vector of arbitrary constants and $\mathbf{H}$ is a $4\times4$ matrix independent of position $x_2$ defined by

$$\mathbf{a} = (A_2^{(1)}, A_2^{(2)}, A_2^{(3)}, A_2^{(4)})^{\mathrm{T}}, \quad \mathbf{H} = \begin{bmatrix} q_1 & -q_1 & q_2 & -q_2 \\ 1 & 1 & 1 & 1 \\ \gamma f(q_1) & \gamma f(q_1) & \gamma f(q_2) & \gamma f(q_2) \\ \gamma q_1 f(q_2) & -\gamma q_1 f(q_2) & \gamma q_2 f(q_1) & -\gamma q_2 f(q_1) \end{bmatrix}, \tag{10}$$

where $f(q_m) = 1 + q_m^2 - \sigma, (m = 1, 2)$ and $\sigma = \sigma_2/\gamma$.

The vector $\mathbf{a}$ is eliminated from Eq. (8) by introducing the vector $\mathbf{y}(\bar{x}_2)$ at some location $x_2 = \bar{x}_2$ to obtain

$$\mathbf{y}(x_2) = \mathbf{H}\mathbf{E}(x_2 - \bar{x}_2)\mathbf{H}^{-1}\mathbf{y}(\bar{x}_2) = \mathbf{P}(x_2 - \bar{x}_2)\mathbf{y}(\bar{x}_2). \tag{11}$$

The matrix $\mathbf{P}(x_2 - \bar{x}_2)$ is the propagator matrix (Gilbert and Backus, 1966; Rogerson and Sandiford, 1997), cf. Appendix A.

## 3. Formulation of the problem

The pre-stressed symmetric layered composite shown in Fig. 1, consists of two isotropic incompressible elastic materials, where the principal axes of strain in each layer are coincident. The Cartesian coordinate system is chosen such that $x_1$- and $x_2$-axes are also coincident with the principal axes, the $x_2$-direction is normal to the free surface of the layered composite, wave propagation is in $x_1$-direction and the origin $O$ lies at the mid plane of the composite. The thickness of the inner layer is $2d$, and the thickness of the outer layers is $h$. The outer layers and inner layer are homogeneous with material parameters and mass density $\alpha$, $\beta$, $\gamma$, $\rho$ and $\alpha^*$, $\beta^*$, $\gamma^*$, $\rho^*$, respectively. In the remainder of the paper, all quantities with an asterisk refer to variables and parameters of the inner layer.

For anti-symmetric wave propagation in the pre-stressed symmetric layered composite it is sufficient to consider only the upper half of the composite ($0 \leqslant x_2 \leqslant d + h$). For the outer layer, from Eq. (11) the relation between displacement–stress increment vectors at the boundary of the layered composite and the interface is written as

$$\mathbf{y}(d + h) = \mathbf{P}(h)\mathbf{y}(d). \tag{12}$$

By considering the displacement and pressure increments for harmonic waves propagating in the $x_1$-direction in the inner layer and introducing the displacement–stress increment vector $\mathbf{y}^*$, the propagator matrix for the inner layer $\mathbf{P}^*$ may be determined. For the inner layer the relation between displacement–stress increment vectors at the interface and mid-plane may be established as

$$\mathbf{y}^*(d) = \mathbf{P}^*(d)\mathbf{y}^*(0). \tag{13}$$

The anti-symmetric mid-plane conditions and the incremental traction free upper surface conditions can be written as

$$U_1^*(0) = S_{022}^*(0) = 0, \qquad S_{021}(d + h) = S_{022}(d + h) = 0. \tag{14}$$

At the interface, stress increments and the displacement increment in the $x_2$-direction are assumed to be continuous, while the shear stress increment is assumed to be proportional to the displacement increment jump in the $x_1$-direction. These interfacial conditions yield

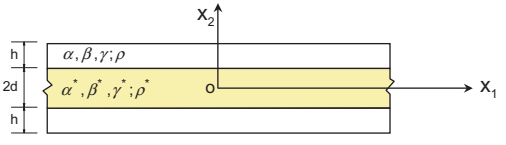


Fig. 1. Pre-stressed equilibrium configuration of a symmetric layered composite.

$$
\begin{aligned}
&S^*_{021}(d) = S_{021}(d), \quad S^*_{022}(d) = S_{022}(d),\\
&U_2(d) = U^*_2(d), \quad S^*_{021}(d) = \frac{k_x\gamma}{h}[U_1(d) - U^*_1(d)],
\end{aligned}
\tag{15}
$$

where $k_x$ is the non-dimensional shear spring parameter. From Eqs. (12), (13) and (15) the relation between $\mathbf{y}(d+h)$ and $\mathbf{y}^*(0)$ is expressed as

$$
\mathbf{y}(d+h) = \mathbf{P}(h)\hat{\mathbf{P}}^*(d)\mathbf{y}^*(0), \tag{16}
$$

where $\hat{P}^*_{ij}(d) = P^*_{ij}(d) + \delta_{i1}khP^*_{3j}(d)/(k_x\gamma)$ and the elements of $\mathbf{P}(h)$ and $\mathbf{P}^*(d)$ are given in Appendix A. Substituting Eq. (14) into Eq. (16) yields a set of four homogeneous linear simultaneous equations for four unknowns from which the dispersion relation for anti-symmetric waves in an imperfectly bonded composite is obtained as

$$
\sum_{i=1}^{4}\sum_{j=1}^{4}[P_{3i}P^*_{i2}P_{4j}P^*_{j3} - P_{3i}P^*_{i3}P_{4j}P^*_{j2}] + \frac{kh}{k_x\gamma}\sum_{i=1}^{4}[P_{3i}P^*_{i2}P_{41}P^*_{33} + P_{4i}P^*_{i3}P_{31}P^*_{32} - P_{3i}P^*_{i3}P_{41}P^*_{32} - P_{4i}P^*_{i2}P_{31}P^*_{33}] = 0, \tag{17}
$$

for $k_x \geqslant 0$, where $P_{ij}$ and $P^*_{ij}$ are the elements of $\mathbf{P}(h)$ and $\mathbf{P}^*(d)$ respectively. The above equation is similar in form to the dispersion relation obtained for symmetric waves (Eq. (3.5), LW, 2003)

$$
\sum_{i=1}^{4}\sum_{j=1}^{4}[P_{3i}P^*_{i1}P_{4j}P^*_{j4} - P_{3i}P^*_{i4}P_{4j}P^*_{j1}] + \frac{kh}{k_x\gamma}\sum_{i=1}^{4}[P_{3i}P^*_{i1}P_{41}P^*_{34} + P_{4i}P^*_{i4}P_{31}P^*_{31} - P_{3i}P^*_{i4}P_{41}P^*_{31} - P_{4i}P^*_{i1}P_{31}P^*_{34}] = 0. \tag{18}
$$

It is seen that the two dispersion relations differ from each other only through the elements $P^*_{ij}$ associated with the inner layer due to the change in mid-plane conditions.

The elements of $\mathbf{P}(h)$ and $\mathbf{P}^*(d)$ are substituted into Eq. (17) and the common factor $q_1q_2(q_1^2 - q_2^2)^2(q_1^{*2} - q_2^{*2})$ is removed from the denominator. The removal of this common factor leads to spurious roots in the resulting relation

$$
\begin{aligned}
&2q_1q_2f(q_1)f(q_2)\Delta_1 + q_1f(q_2)^2[C_1S_2\Delta_2 + C_1C_2\Delta_3 + S_1S_2\Delta_4 + S_1C_2\Delta_5] - q_2f(q_1)^2[S_1C_2\Delta_2\\
&\quad + S_1S_2\Delta_3 + C_1C_2\Delta_4 + C_1S_2\Delta_5] + \left(\frac{kh}{k_x}\right)\{q_1f(q_2)^2[C_1S_2\Delta_6 + S_1S_2\Delta_7 + (C_1C_2 - 1)\Delta_8]\\
&\quad - q_2f(q_1)^2[S_1C_2\Delta_6 + (C_1C_2 - 1)\Delta_7 + S_1S_2\Delta_8]\} = 0,
\end{aligned}
\tag{19}
$$

where

$$
\begin{aligned}
\Delta_1 &= q^*_1[f^*(q^*_2) - rf(q_2)][rf(q_1) - f^*(q^*_2)]S^*_1C^*_2 + q^*_2[f^*(q^*_1) - rf(q_2)][f^*(q^*_1) - rf(q_1)]C^*_1S^*_2,\\
\Delta_2 &= q^*_1q^*_2r[f(q_1) - f(q_2)][f^*(q^*_1) - f^*(q^*_2)]S^*_1S^*_2,\\
\Delta_3 &= q^*_1q_2[f^*(q^*_2) - rf(q_1)]^2S^*_1C^*_2 - q^*_2q_2[f^*(q^*_1) - rf(q_1)]^2C^*_1S^*_2,\\
\Delta_4 &= q^*_2q_1[f^*(q^*_1) - rf(q_2)]^2C^*_1S^*_2 - q^*_1q_1[f^*(q^*_2) - rf(q_2)]^2S^*_1C^*_2,\\
\Delta_5 &= q_1q_2r[f(q_1) - f(q_2)][f^*(q^*_1) - f^*(q^*_2)]C^*_1C^*_2,\\
\Delta_6 &= [f(q_1) - f(q_2)][q^*_2f^*(q^*_1)^2C^*_1S^*_2 - q^*_1f^*(q^*_2)^2S^*_1C^*_2],\\
\Delta_7 &= q_1rf(q_2)^2[f^*(q^*_2) - f^*(q^*_1)]C^*_1C^*_2,\\
\Delta_8 &= q_2rf(q_1)^2[f^*(q^*_1) - f^*(q^*_2)]C^*_1C^*_2,
\end{aligned}
\tag{20}
$$

and $f(q_m)$, $C_m$, $S_m$, $(m = 1, 2)$ are defined in Eq. (A.2) and $f^*(q_m^*)$, $C_m^*$, $S_m^*$, $(m = 1, 2)$, $r$ are defined in Eq. (A.3). Eq. (19) is identical to the dispersion relation for symmetric waves (Eq. (3.6), LW, 2003) but $\Delta_i$, $(i = 1, 2, \ldots, 8)$ for the present case (Eq. (20)) is obtained by replacing $C_m^*$ by $S_m^*$ and $S_m^*$ by $C_m^*$, $(m = 1, 2)$ in Eq. (3.7) of LW (2003). Rogerson and Sandiford (1997) obtained the dispersion relation in a similar form for the perfectly bonded case.

Eq. (19) can be written in a more compact form as

$$\begin{aligned} &q_1^* S_1^* C_2^* [f^*(q_2^*)^2 \Delta_9 + f^*(q_2^*)\Delta_{10} + \Delta_{11}] - q_2^* C_1^* S_2^* [f^*(q_1^*)^2 \Delta_9 + f^*(q_1^*)\Delta_{10} + \Delta_{11}] \\ &\quad - [f^*(q_1^*) - f^*(q_2^*)][q_1^* q_2^* S_1^* S_2^* \Delta_{12} + C_1^* C_2^* \Delta_{13}] + \left(\frac{kh}{rk_x}\right)\{[f^*(q_1^*) - f^*(q_2^*)]C_1^* C_2^* \Delta_{11} \\ &\quad + [q_1^* f^*(q_2^*)^2 S_1^* C_2^* - q_2^* f^*(q_1^*)^2 C_1^* S_2^*]\Delta_{12}\} = 0, \end{aligned} \tag{21}$$

where

$$\begin{aligned} \Delta_9 &= 2q_1 q_2 f(q_1) f(q_2) - q_1 q_2 [f(q_1)^2 + f(q_2)^2] C_1 C_2 + [q_1^2 f(q_2)^2 + q_2^2 f(q_1)^2] S_1 S_2, \\ \Delta_{10} &= 2r\{q_1 q_2 f(q_1) f(q_2)[f(q_1) + f(q_2)](C_1 C_2 - 1) - [q_1^2 f(q_2)^3 + q_2^2 f(q_1)^3] S_1 S_2\}, \\ \Delta_{11} &= r^2\{-2q_1 q_2 f(q_1)^2 f(q_2)^2 (C_1 C_2 - 1) + [q_1^2 f(q_2)^4 + q_2^2 f(q_1)^4] S_1 S_2\}, \\ \Delta_{12} &= r[f(q_1) - f(q_2)][q_1 f(q_2)^2 C_1 S_2 - q_2 f(q_1)^2 S_1 C_2], \\ \Delta_{13} &= r q_1 q_2 [f(q_1) - f(q_2)][q_1 f(q_2)^2 S_1 C_2 - q_2 f(q_1)^2 C_1 S_2]. \end{aligned} \tag{22}$$

The corresponding equation for symmetric waves (Eq. (3.8), LW, 2003) can be obtained from Eq. (21) by replacing $C_m^*$ by $S_m^*$ and $S_m^*$ by $C_m^*$, $(m = 1, 2)$, and Eq. (3.9) of LW (2003) is the same as Eq. (22). It is noted that other than the term $r = \gamma/\gamma^*$ all terms in Eq. (22) are related only to the outer layer.

When $k_x \to \infty$ the dispersion relation for a perfectly bonded interface is obtained from Eq. (19) as

$$\begin{aligned} &2q_1 q_2 f(q_1) f(q_2) \Delta_1 + q_1 f(q_2)^2 [C_1 S_2 \Delta_2 + C_1 C_2 \Delta_3 + S_1 S_2 \Delta_4 + S_1 C_2 \Delta_5] \\ &\quad - q_2 f(q_1)^2 [S_1 C_2 \Delta_2 + S_1 S_2 \Delta_3 + C_1 C_2 \Delta_4 + C_1 S_2 \Delta_5] = 0, \end{aligned} \tag{23}$$

and from Eq. (21) as

$$\begin{aligned} &q_1^* S_1^* C_2^* [f^*(q_2^*)^2 \Delta_9 + f^*(q_2^*)\Delta_{10} + \Delta_{11}] - q_2^* C_1^* S_2^* [f^*(q_1^*)^2 \Delta_9 + f^*(q_1^*)\Delta_{10} + \Delta_{11}] \\ &\quad - [f^*(q_1^*) - f^*(q_2^*)][q_1^* q_2^* S_1^* S_2^* \Delta_{12} + C_1^* C_2^* \Delta_{13}] = 0. \end{aligned} \tag{24}$$

The expression given in Eq. (3.7) of Rogerson and Sandiford (1997) for the perfectly bonded case contains some minor errors.

When $k_x = 0$ the dispersion relation for the fully slipping interface is obtained from Eq. (19) as

$$q_1 f(q_2)^2 [C_1 S_2 \Delta_6 + S_1 S_2 \Delta_7 + (C_1 C_2 - 1)\Delta_8] - q_2 f(q_1)^2 [S_1 C_2 \Delta_6 + (C_1 C_2 - 1)\Delta_7 + S_1 S_2 \Delta_8] = 0, \tag{25}$$

and from Eq. (21) as

$$[f^*(q_1^*) - f^*(q_2^*)] C_1^* C_2^* \Delta_{11} + [q_1^* f^*(q_2^*)^2 S_1^* C_2^* - q_2^* f^*(q_1^*)^2 C_1^* S_2^*]\Delta_{12} = 0. \tag{26}$$

It is noted that Eqs. (23) or (24) and (25) or (26) can also be obtained directly by separately considering the perfectly bonded interface problem (Rogerson and Sandiford, 1997) and the slipping interface problem.

## 4. Analysis of dispersion relation

The similarity of the dispersion relations for anti-symmetric and symmetric waves shown in Section 3, results in similar behavior for these two kinds of waves, which will be discussed in this section. The roots $q_1^2$, $q_2^2$ of Eq. (4) can be written as

$$q_1^2, q_2^2 = \frac{1}{2}\left[2\bar{\beta} - \xi \mp \sqrt{(2\bar{\beta} - \xi)^2 - 4(\bar{\alpha} - \xi)}\right], \tag{27}$$

where $\xi = \rho v^2/\gamma$ is the non-dimensional square of the phase speed and $\bar{\alpha} = \alpha/\gamma$, $\bar{\beta} = \beta/\gamma$. Similar expressions for $q_1^{*2}$ and $q_2^{*2}$, for the inner layer are

$$q_1^{*2}, q_2^{*2} = \frac{1}{2}\left[2\bar{\beta}^* - \xi^* \mp \sqrt{(2\bar{\beta}^* - \xi^*)^2 - 4(\bar{\alpha}^* - \xi^*)}\right], \tag{28}$$

where $\bar{\alpha}^* = \alpha^*/\gamma^*$, $\bar{\beta}^* = \beta^*/\gamma^*$, $\xi^* = \rho^* v^2/\gamma^* = a\xi$ and $a = r\rho^*/\rho$. For brevity, in what follows the non-dimensional square of the phase speed $\xi$ is referred to as *squared phase speed*.

In the present paper, the common factor $q_1 q_2 (q_1^2 - q_2^2)^2 (q_1^{*2} - q_2^{*2})$ taken out from the denominator of Eq. (17) leads to spurious roots of Eq. (21) given by

$$\begin{aligned}
&\xi = \xi_{S1} = \bar{\alpha}, && \text{when} \quad q_1 = 0 \text{ or } q_2 = 0,\\
&\xi = \xi_{S2}, \xi_{S3} = 2(\bar{\beta} - 1 \pm \sqrt{\bar{\alpha} - 2\bar{\beta} + 1}), && \text{when} \quad q_1^2 = q_2^2,\\
&\xi^* = \xi^*_{S2}, \xi^*_{S3} = 2(\bar{\beta}^* - 1 \pm \sqrt{\bar{\alpha}^* - 2\bar{\beta}^* + 1}), && \text{when} \quad q_1^{*2} = q_2^{*2}.
\end{aligned} \tag{29}$$

This is in contrast to the case of symmetric waves, which has a common factor $q_1 q_2 q_1^* q_2^* (q_1^2 - q_2^2)^2 (q_1^{*2} - q_2^{*2})$ with an additional spurious root at $\xi^* = \xi^*_{S1} = \bar{\alpha}^*$ (when $q_1^* q_2^* = 0$). Here $\xi_{S1}$ and $\xi_{S2}$ ($\xi^*_{S1}$ and $\xi^*_{S2}$) are upper bounds on the squared phase speed of pure surface waves propagating in a half space of the outer layer (inner layer) material (Ogden and Sotiropoulos, 1995).

### 4.1. Low wavenumber limit $kh \to 0$

When $kh \to 0$ the thickness of the layers are very small compared to the wavelength. By considering small argument expansions of the hyperbolic functions, the squared phase speeds for the imperfect interface and perfectly bonded cases are obtained from Eqs. (21) and (24) as

$$\xi_0^{(A)} = \frac{D[\bar{\alpha}^* - (1 - r\sigma)^2] + r[\bar{\alpha} - (1 - \sigma)^2]}{aD + r}, \tag{30a}$$

and for the fully slipping case from Eq. (26) as

$$\xi_{01}^{(A)} = 2(\bar{\beta} + 1 - \sigma), \qquad \xi_{02}^{(A)} = \xi_0^{(A)}. \tag{30b}$$

The finite squared phase speed $\xi_0^{(A)}$ agrees with Eq. (4.2) of Rogerson and Sandiford (1997) while $\xi_{01}^{(A)}$ corresponds to the fundamental mode of symmetric waves of an incompressible elastic layer with free surfaces (see Eq. (4.5), Rogerson, 1997). The corresponding results for symmetric waves are (LW, 2003),

$$\begin{aligned}
&\xi_0^{(S)} = \frac{2[D(\bar{\beta}^* + 1 - r\sigma) + r(\bar{\beta} + 1 - \sigma)]}{aD + r},\\
&\xi_{01}^{(S)} = 2(\bar{\beta} + 1 - \sigma), \qquad \xi_{02}^{(S)} = 2(\bar{\beta}^* + 1 - r\sigma)/a.
\end{aligned} \tag{31}$$

Here it is seen that $\xi_{01}^{(A)} = \xi_{01}^{(S)}$. This has been verified by examining the displacement profiles of the composite. At this squared phase speed, for anti-symmetric waves $u_1 =$ constant and $u_2 \to 0$ in the upper outer layer (and the lower outer layer moves in the opposite direction) while $u_1, u_2 \to 0$ for the inner layer; for

symmetric wave $u_1 =$ constant and $u_2 \to 0$ in the upper outer layer (and the lower outer layer moves in the same direction) while $u_1, u_2 \to 0$ for the inner layer. In addition for anti-symmetric waves $\xi_{02}^{(A)} = \xi_0^{(A)}$ and now $u_1 \to 0$ and $u_2 =$ constant for all layers.

Eqs. (30) and (31) are the finite squared phase speeds of the lowest branches of the dispersion curves, which have frequencies that tend to zero as $kh \to 0$. The frequencies of higher modes which have infinite squared phase speeds ($\xi \to \infty$) when $kh \to 0$ are considered next. When $\xi \to \infty$ expressions for $q_1^2$, $q_2^2$, $q_1^{*2}$ and $q_2^{*2}$ can be obtained from Eqs. (27) and (28) as

$$\begin{aligned} q_1^2 &= -\xi + 2\bar{\beta} - 1 - \frac{2\bar{\beta} - \bar{\alpha} - 1}{\xi} + O(\xi^{-2}), \quad q_2^2 = 1 + \frac{2\bar{\beta} - \bar{\alpha} - 1}{\xi} + O(\xi^{-2}), \\ q_1^{*2} &= -a\xi + 2\bar{\beta}^* - 1 - \frac{2\bar{\beta}^* - \bar{\alpha}^* - 1}{a\xi} + O(\xi^{-2}), \quad q_2^{*2} = 1 + \frac{2\bar{\beta}^* - \bar{\alpha}^* - 1}{a\xi} + O(\xi^{-2}). \end{aligned} \tag{32}$$

It is easily seen that $q_1$, $q_1^*$ are imaginary while $q_2$, $q_2^*$ are real. By substituting Eq. (32) into Eq. (21), introducing the non-dimensional frequency parameter $\Omega = kh\sqrt{\xi}$ and considering small argument expansions of the hyperbolic functions, the expression to determine the cut-off frequencies ($\Omega_C^{(A)} > 0$) is obtained as

$$\sqrt{a}\Omega_C^{(A)} \sin(\Omega_C^{(A)}) \cos(\sqrt{a}D\Omega_C^{(A)}) - k_x[\sqrt{a}\cos(\Omega_C^{(A)}) \cos(\sqrt{a}D\Omega_C^{(A)}) - r\sin(\Omega_C^{(A)}) \sin(\sqrt{a}D\Omega_C^{(A)})] = 0. \tag{33}$$

Similar to the case of symmetric waves (LW, 2003) the cut-off frequencies obtained from Eq. (33) depend only on the non-dimensional parameters $a$, $D$, $r$ and $k_x$ and the equations for cut-off frequencies of the perfectly bonded and fully slipping cases may also be deduced from this equation. For the fully slipping interface $\Omega_C^{(A)} = n\pi$, $(n - \frac{1}{2})\pi/(\sqrt{a}D)$, $(n = 1, 2, \ldots)$ where $n\pi$ corresponds to the cut-off frequencies for symmetric waves propagating in the outer layer with free surfaces, and $(n - \frac{1}{2})\pi/(\sqrt{a}D)$ corresponds to the cut-off frequencies for anti-symmetric waves propagating in the inner layer with free surfaces (see Eqs. (3.8c) and (3.13c), Kaplunov et al., 2002).

### 4.2. High wavenumber limit $kh \to \infty$

When $kh \to \infty$ the thickness of the layers are very large compared to wavelength and the propagation behavior is similar to waves in a semi-infinite medium and two joined semi-infinite media. Hence for both anti-symmetric and symmetric wave propagation the same high wavenumber limits are expected. The behavior of the dispersion relation in this region depends on the roots $q_1$, $q_2$, $q_1^*$ and $q_2^*$ which may either real, pure imaginary or complex conjugates which in turn depends on squared phase speed $\xi$ and the parameters $\bar{\alpha}$, $\bar{\beta}$, $\bar{\alpha}^*$, $\bar{\beta}^*$ (see Appendix B).

#### 4.2.1. Roots $q_1$, $q_2$, $q_1^*$ and $q_2^*$ are real or complex conjugates with non-zero real part

When $kh \to \infty$, hyperbolic functions in the dispersion relation $C_m$, $S_m$, $C_m^*$ and $S_m^* \to \infty$, $(m = 1, 2)$. For anti-symmetric waves in the case of an imperfectly bonded interface, dividing Eq. (21) by $C_1C_2C_1^*C_2^*$, taking the limit $kh \to \infty$ and removing the common factor $(q_1 - q_2)^2(q_1^* - q_2^*)$, yields

$$R_\sigma(\xi) I_S(\xi) = 0, \tag{34}$$

where $R_\sigma(\xi) = 0$ and $I_S(\xi) = 0$ are the secular equations for the squared phase speeds of the Rayleigh surface wave of the outer layer (Dowaikh and Ogden, 1990) and the Stoneley interfacial wave for fully slipping half spaces given by

$$R_\sigma(\xi) = \eta^3 + \eta^2 + (2 - 2\sigma + 2\bar{\beta} - \bar{\alpha})\eta - (1 - \sigma)^2, \tag{35}$$

$$I_S(\xi) = (q_1 + q_2)R^*_\sigma(\xi) + r(q^*_1 + q^*_2)R_\sigma(\xi), \tag{36}$$

in which

$$R^*_\sigma(\xi) = \eta^{*3} + \eta^{*2} + (2 - 2r\sigma + 2\bar{\beta}^* - \bar{\alpha}^*)\eta^* - (1 - r\sigma)^2, \tag{37}$$

where $\eta = \sqrt{\bar{\alpha} - \xi}$ and $\eta^* = \sqrt{\bar{\alpha}^* - a\xi}$.

Similarly analyzing Eqs. (24) and (26) yields

$$R_\sigma(\xi)I_P(\xi) = 0, \tag{38}$$

for the perfectly bonded interface and Eq. (34) for the fully slipping interface, where $I_P(\xi) = 0$, is the secular equation for the squared phase speed of Stoneley interfacial waves for perfectly bonded half spaces (Dowaikh and Ogden, 1991) given by

$$I_P(\xi) = r^2R_0(\xi) + R^*_0(\xi) + 2r(1 - q_1q_2)(1 - q^*_1q^*_2) + r(q_1 + q_2)(q^*_1 + q^*_2)(q_1q_2 + q^*_1q^*_2) = 0. \tag{39}$$

In the above equation, $R_0(\xi)$ and $R^*_0(\xi)$ are the Rayleigh wave equations (see Eqs. (35) and (37)) with zero Cauchy stress ($\sigma = 0$).

Eqs. (34) and (38) were also obtained for the symmetric wave case in LW (2003). The roots of Eqs. (35), (36) and (39) (presented in different forms in Eqs. (4.10) and (4.12) of LW (2003)) are denoted by $\xi_R$, $\xi_{IS}$ and $\xi_{IP}$, respectively. In addition, Eq. (36) when there is no pre-stress, agrees with the secular equation of slip-waves propagating in two different linear isotropic half-spaces in sliding contact (see Eq. (23), Barnett et al., 1988).

*4.2.2. At least one of the roots $q_1$, $q_2$, $q^*_1$ and $q^*_2$ is pure imaginary*

When $kh \to \infty$ the hyperbolic functions $C_m$, $S_m$, $C^*_m$ and $S^*_m$, $(m = 1, 2)$ with pure imaginary arguments are finite and the dispersion relation Eq. (21) yields for all values of $k_x$ squared phase speeds $\xi$ that will tend to the limiting squared phase speed of the bi-material composite $\xi_{CL}$ (Rogerson and Sandiford, 2000), given by

$$\xi_{CL} = \min(\xi_L, \xi^*_L/a), \tag{40}$$

where

$$\xi_L = \begin{cases} \xi_{S1} = \bar{\alpha}; & \bar{\alpha} \leqslant 2\bar{\beta} \\ \xi_{S2} = 2(\bar{\beta} - 1 + \sqrt{\bar{\alpha} - 2\bar{\beta} + 1}); & \bar{\alpha} > 2\bar{\beta} \end{cases} \quad \text{(for outer layers)}, \tag{41a}$$

$$\xi^*_L = \begin{cases} \xi^*_{S1} = \bar{\alpha}^*; & \bar{\alpha}^* \leqslant 2\bar{\beta}^* \\ \xi^*_{S2} = 2(\bar{\beta}^* - 1 + \sqrt{\bar{\alpha}^* - 2\bar{\beta}^* + 1}); & \bar{\alpha}^* > 2\bar{\beta}^* \end{cases} \quad \text{(for inner layer)}, \tag{41b}$$

where $\xi_L$ and $\xi^*_L$ are limiting squared phase speeds of the outer layers and the inner layer, respectively. Hence, there are four possible cases of limiting squared phase speeds of the composite, Case 1: $\xi_{CL} = \xi_{S1}$; Case 2: $\xi_{CL} = \xi_{S2}$; Case 3: $\xi_{CL} = \xi^*_{S1}/a$ and Case 4: $\xi_{CL} = \xi^*_{S2}/a$.

Comparing Eqs. (34)–(41) with Section 4.2 of LW (2003) it is seen that the limiting squared phase speeds when $kh \to \infty$ for anti-symmetric and symmetric waves are the same. In the case of anti-symmetric waves, the squared phase speed of the fundamental mode and the next higher modes are denoted $\xi^{(1)}_A$ and $\xi^{(n)}_A$ $(n = 2, 3, \ldots)$, and for symmetric waves, the squared phase speed of the fundamental mode and the next higher modes are denoted as $\xi^{(1)}_S$ and $\xi^{(n)}_S$ $(n = 2, 3, \ldots)$, respectively. Hence, the limiting squared phase speeds when $kh \to \infty$ for the case of a perfectly bonded interface will be given by

$$\begin{aligned}
&\xi_{\mathrm{A}}^{(1)}, \xi_{\mathrm{S}}^{(1)} \to \min(\xi_{\mathrm{R}}, \xi_{\mathrm{IP}}), \quad \xi_{\mathrm{A}}^{(2)}, \xi_{\mathrm{S}}^{(2)} \to \max(\xi_{\mathrm{R}}, \xi_{\mathrm{IP}}), \quad \xi_{\mathrm{A}}^{(n)}, \xi_{\mathrm{S}}^{(n)} \to \xi_{\mathrm{CL}}, \\
&\quad n = 3, 4, \ldots, \text{ when both } \xi_{\mathrm{R}}, \xi_{\mathrm{IP}} < \xi_{\mathrm{CL}}; \\
&\xi_{\mathrm{A}}^{(1)}, \xi_{\mathrm{S}}^{(1)} \to \xi_{\mathrm{R}}, \quad \xi_{\mathrm{A}}^{(n)}, \xi_{\mathrm{S}}^{(n)} \to \xi_{\mathrm{CL}}, \quad n = 2, 3, \ldots, \text{ when only } \xi_{\mathrm{R}} < \xi_{\mathrm{CL}}; \\
&\xi_{\mathrm{A}}^{(1)}, \xi_{\mathrm{S}}^{(1)} \to \xi_{\mathrm{IP}}, \quad \xi_{\mathrm{A}}^{(n)}, \xi_{\mathrm{S}}^{(n)} \to \xi_{\mathrm{CL}}, \quad n = 2, 3, \ldots, \text{ when only } \xi_{\mathrm{IP}} < \xi_{\mathrm{CL}}; \\
&\xi_{\mathrm{A}}^{(n)}, \xi_{\mathrm{S}}^{(n)} \to \xi_{\mathrm{CL}}, \quad n = 1, 2, \ldots, \text{ when } \xi_{\mathrm{R}} \geqslant \xi_{\mathrm{CL}} \text{ and } \xi_{\mathrm{IP}} \text{ does not exist or when both} \\
&\quad \xi_{\mathrm{R}}, \xi_{\mathrm{IP}} \text{ do not exist.}
\end{aligned} \tag{42}$$

For the fully slipping and the imperfect interface cases, the squared phase speed $\xi_{\mathrm{IP}}$ above is replaced by $\xi_{\mathrm{IS}}$.

## 5. Stability considerations

In this section, stability issues for both anti-symmetric and symmetric waves are discussed, as the latter case was not considered in LW (2003). For a particular mode when $\xi < 0$, the phase speed $v$ is pure imaginary and instead of harmonic waves travelling in the $x_1$-direction, the displacement and pressure increments given by Eq. (3) will correspond to standing waves with amplitudes that grow exponentially with time, i.e., an *unstable* state. Harmonic waves travelling in the $x_1$-direction will be *stable* for a particular mode when $\xi > 0$, while $\xi = 0$ corresponds to the *neutral* state where static modes of incremental deformation occur. For a given pre-stressed state the layered composite can be considered to be stable for wave propagation in $x_1$-direction, if the squared phase speed $\xi$ of all branches are positive for all $kh$.

The strong ellipticity conditions (Eq. (6)) for the outer and inner layer materials yield the inequalities,

$$\bar{\alpha} > 0, \quad \bar{\beta} > -\sqrt{\bar{\alpha}}; \quad \bar{\alpha}^* > 0, \quad \bar{\beta}^* > -\sqrt{\bar{\alpha}^*}. \tag{43}$$

Considering the limiting squared phase speeds when $kh \to \infty$ given by Eqs. (40)–(41) together with Eq. (43), yields that $\xi_{\mathrm{CL}} > 0$. As noted earlier in Section 4.2.2 since the branches of the dispersion curves (which may or may not include the lowest modes) tend to $\xi_{\mathrm{CL}}$ when $kh \to \infty$, if the inequalities given by Eq. (43) is violated, unstable modes will exist. However, since the squared phase speed of the lowest modes could be less than $\xi_{\mathrm{CL}}$, satisfying the inequality given by Eq. (43) does not guarantee that all modes will be stable, i.e., the strong ellipticity condition is necessary but insufficient for stable wave propagation.

The *bifurcation equation* is obtained from the dispersion relation by setting the squared phase speed $\xi$ to zero and yields the *neutral curves* that separate the stable and unstable regions associated with the fundamental mode or the next lowest mode. Substituting $\xi = 0$ into Eq. (17) for anti-symmetric waves and Eq. (18) for symmetric waves, two quartic equations

$$\Phi_4^{(\mathrm{A})}\sigma^4 + \Phi_3^{(\mathrm{A})}\sigma^3 + \Phi_2^{(\mathrm{A})}\sigma^2 + \Phi_1^{(\mathrm{A})}\sigma + \Phi_0^{(\mathrm{A})} = 0, \tag{44a}$$

$$\Phi_4^{(\mathrm{S})}\sigma^4 + \Phi_3^{(\mathrm{S})}\sigma^3 + \Phi_2^{(\mathrm{S})}\sigma^2 + \Phi_1^{(\mathrm{S})}\sigma + \Phi_0^{(\mathrm{S})} = 0, \tag{44b}$$

are obtained, where $\Phi_n^{(\mathrm{A})}$ and $\Phi_n^{(\mathrm{S})}$ are functions of $\bar{\alpha}$, $\bar{\beta}$, $\bar{\alpha}^*$, $\bar{\beta}^*$, $kh$, $k_x$, $r$, $a$ and $D$. For the perfectly bonded case, the bifurcation equations given by Eq. (44) reduce to quadratic equations (see Eq. (6.1) of Rogerson and Sandiford (1997) for anti-symmetric waves and Eq. (5.1) of Rogerson and Sandiford (1996) for symmetric waves), while for the fully slipping interface case, Eqs. (44a) and (44b) remain as quartic equations.

### 5.1. Stable range of $\sigma$ as $kh \to 0$

The solutions of Eq. (44) as $kh \to 0$ can be computed directly from Eqs. (44) but are readily obtained from Eqs. (30) and (31) with the squared phase speed set to zero.

For anti-symmetric wave propagation in an imperfectly bonded or perfectly bonded layered composite, from Eq. (30a) the stable range for $\xi_0^{(A)} > 0$ can be obtained as

$$\sigma_0^{-(A)} < \sigma < \sigma_0^{+(A)}, \tag{45}$$

where

$$\sigma_0^{+(A)}, \sigma_0^{-(A)} = \frac{1+D}{1+rD} \pm \sqrt{\frac{r\bar{\alpha} + D\bar{\alpha}^*}{r(1+rD)} - \frac{D}{r}\left(\frac{1-r}{1+rD}\right)^2}. \tag{46}$$

For the fully slipping interface case from Eq. (30b) the stable range for $\xi_{01}^{(A)} > 0$ and $\xi_{02}^{(A)} > 0$ is

$$\sigma_{02}^{-(A)} < \sigma < \min(\sigma_{01}^{(A)}, \sigma_{02}^{+(A)}), \tag{47}$$

where

$$\sigma_{01}^{(A)} = \bar{\beta} + 1, \qquad \sigma_{02}^{+(A)} = \sigma_0^{+(A)}, \qquad \sigma_{02}^{-(A)} = \sigma_0^{-(A)}. \tag{48}$$

In addition, if $\sigma > \max(\sigma_{01}^{(A)}, \sigma_{02}^{+(A)})$ then both $\xi_{01}^{(A)}$ and $\xi_{02}^{(A)}$ are negative.

It is seen from Eq. (46) that if there is no real value of $\sigma_0^{\pm(A)}$ i.e., when

$$\frac{r\bar{\alpha} + D\bar{\alpha}^*}{r(1+rD)} - \frac{D}{r}\left(\frac{1-r}{1+rD}\right)^2 < 0, \tag{49}$$

then from Eq. (30a) it can be shown that

$$\xi_0^{(A)} < \frac{-r[1-\sigma+D(1-r\sigma)]^2}{(1+rD)(aD+r)} \leqslant 0, \tag{50}$$

and hence for all $k_x$ one of the lowest modes will be unstable.

For symmetric waves, in an imperfectly bonded or perfectly bonded layered composite, from Eq. (31a) the stable range for $\xi_0^{(S)} > 0$ is

$$\sigma < \sigma_0^{(S)}, \tag{51}$$

where

$$\sigma_0^{(S)} = \frac{D(\bar{\beta}^* + 1) + r(\bar{\beta} + 1)}{r(1+D)}. \tag{52}$$

For the fully slipping interface case, Eq. (31b) yields the stable range of $\sigma$ for $\xi_{01}^{(S)} > 0$ and $\xi_{02}^{(S)} > 0$ is

$$\sigma < \min(\sigma_{01}^{(S)}, \sigma_{02}^{(S)}), \tag{53}$$

where

$$\sigma_{01}^{(S)} = \sigma_{01}^{(A)}, \qquad \sigma_{02}^{(S)} = (\bar{\beta}^* + 1)/r. \tag{54}$$

Similar to the anti-symmetric wave case i.e., if $\sigma > \max(\sigma_{01}^{(S)}, \sigma_0^{(S)})$ then $\xi_{01}^{(S)} < 0$ and $\xi_{02}^{(S)} < 0$.

### 5.2. Stable range of $\sigma$ as $kh \to \infty$

The limiting squared phase speeds for both symmetric and anti-symmetric waves as $kh \to \infty$ are the same, i.e., $\xi_R$, $\xi_{IP}$ or $\xi_{CL}$ for perfectly bonded interface case and $\xi_R$, $\xi_{IS}$ or $\xi_{CL}$ for imperfectly bonded and fully slipping interface cases (see Section 4.2). However, for composites which already satisfy the strong ellipticity conditions, $\xi_{CL}$ is always positive and the secular equation used to obtain $\xi_{IP}$ does not depend on $\sigma$, therefore the stable ranges of $\sigma$ as $kh \to \infty$ may be computed by just considering Eq. (35) for perfectly bonded case, and considering Eqs. (35) and (36) for imperfectly bonded and fully slipping interface cases only.

For the perfectly bonded interface case, from Eq. (35) the stable range for $\xi_R > 0$ is

$$\sigma_R^- < \sigma < \sigma_R^+, \tag{55}$$

where

$$\sigma_R^+, \sigma_R^- = 1 - \sqrt{\bar{\alpha}} \pm \sqrt{2\bar{\alpha} + 2\bar{\beta}\sqrt{\bar{\alpha}}}. \tag{56}$$

This is the required range of values of $\sigma$ for the existence of a unique surface wave in an incompressible elastic half-space (see Eq. (6.13) of Dowaikh and Ogden (1990)).

While for the fully slipping and the imperfect interfaces cases, the stable range for non-negative values of $\xi_R$ and $\xi_{IS}$ should be

$$\max(\sigma_R^-, \sigma_{IS}^-) < \sigma < \min(\sigma_R^+, \sigma_{IS}^+), \tag{57}$$

where

$$\sigma_{IS}^+, \sigma_{IS}^- = \frac{\zeta(1-\sqrt{\bar{\alpha}^*}) + \zeta^*(1-\sqrt{\bar{\alpha}})}{r\zeta + \zeta^*} \pm \left\{ \left[ \frac{\zeta(1-\sqrt{\bar{\alpha}^*}) + \zeta^*(1-\sqrt{\bar{\alpha}})}{r\zeta + \zeta^*} \right]^2 - \left[ \frac{\zeta\sigma_R^{*+}\sigma_R^{*-} + r\zeta^*\sigma_R^+\sigma_R^-}{r(r\zeta + \zeta^*)} \right] \right\}^{\frac{1}{2}}, \tag{58}$$

and

$$\zeta = \sqrt{\bar{\beta} + \sqrt{\bar{\alpha}}}, \qquad \zeta^* = \sqrt{\bar{\beta}^* + \sqrt{\bar{\alpha}^*}}, \qquad \sigma_R^{*+}, \sigma_R^{*-} = 1 - \sqrt{\bar{\alpha}^*} \pm \sqrt{2\bar{\alpha}^* + 2\bar{\beta}^*\sqrt{\bar{\alpha}^*}}.$$

It can be shown that when there is no real value of $\sigma_{IS}^{\pm}$ that $\xi_{IS} < 0$ and one of the lowest modes will be unstable.

## 6. Numerical results

The examples discussed in this section correspond to the four examples considered for symmetric waves in LW (2003), where incompressible elastic materials with Mooney–Rivlin and Varga strain energy functions were used.

The strain energy function $W^{(MR)}$ of Mooney–Rivlin material (Ogden and Sotiropoulos, 1997) is

$$W^{(MR)} = \frac{1}{2}\mu_1(\lambda_1^2 + \lambda_2^2 + \lambda_3^2 - 3) + \frac{1}{2}\mu_2(\lambda_1^{-2} + \lambda_2^{-2} + \lambda_3^{-2} - 3), \tag{59}$$

where $\mu_1$ and $\mu_2$ are material constants. Using Eq. (5) the parameters $\bar{\alpha}$ and $\bar{\beta}$ of this material are expressed as

$$\bar{\alpha} = \lambda_1^2/\lambda_2^2, \qquad 2\bar{\beta} = \bar{\alpha} + 1. \tag{60}$$

The strain energy function $W^{(V)}$ of Varga material (Ogden and Sotiropoulos, 1997) is

$$W^{(V)} = 2\mu(\lambda_1 + \lambda_2 + \lambda_3 - 3), \tag{61}$$

where $\mu$ is a material constant and from Eq. (5) the parameters $\bar{\alpha}$ and $\bar{\beta}$ of this material are given by

$$\bar{\alpha} = \lambda_1^2/\lambda_2^2, \qquad \bar{\beta} = \lambda_1/\lambda_2. \tag{62}$$

The parameters $\bar{\alpha}^*$ and $\bar{\beta}^*$ for the inner layer are similarly obtained.

The dispersion curves can be obtained either by solving Eq. (21) and disregarding non-dispersive spurious roots (see Eq. (29)), or directly from Eq. (17), where when $\xi$ is equal to any spurious root, l'Hôpital's rule is employed. Here the latter method is used to obtain the dispersion curves. In the case of dispersion curves the results for symmetric waves are only plotted for comparison purposes and the discussion is mostly regarding anti-symmetric waves.

The neutral curves are plotted from Eqs. (44). But when the numerator and denominator of each coefficient $\Phi_i^{(A,S)} (i = 0, \ldots, 4)$ vanish (which corresponds to a spurious root $\xi = 0$ in Eq. (29)) l'Hôpital's rule is used to obtain the neutral curves. For example, it can be shown from Eq. (29) that either $\xi_{S2} = 0$ or $\xi_{S3} = 0$ when $\bar{\alpha} = \bar{\beta}^2$, which occurs for Varga material and which also occurs for the equi-biaxial deformation state for any material where $\bar{\alpha} = \bar{\beta} = 1$. As mentioned in Section 5, Eqs. (44) reduces to quadratic equations for the case of a perfectly bonded interface, hence at most two neutral curves may exist; while for the fully slipping and imperfect interface cases at most four neutral curves may exist.

In Examples 1–4 for a given state of pre-stress the parameters $\bar{\alpha}$, $\bar{\beta}$, $\bar{\alpha}^*$, $\bar{\beta}^*$ are computed while the non-dimensional parameters $r$, $a$, $\sigma$, $k_x$ and $D$ are prescribed. For each example the shear spring parameter is prescribed as $k_x = 0, 1$ and $\infty$, and the squared phase speeds of the first sixteen modes $\xi_A^{(n)}$ and $\xi_S^{(n)}$, $(n = 1, 2, \ldots, 16)$ are plotted in semi-log scale to clearly show the low wavenumber limits. In addition to examine the cut-off frequencies the frequencies of the first sixteen modes $\Omega_A^{(n)}$ and $\Omega_S^{(n)}$, $(n = 1, 2, \ldots, 16)$ are also plotted. The limiting squared phase speeds calculated from Eqs. (30), (31), (35)–(37), (39) and (41) are given in Table 1. Stability issues are explored by plotting neutral curves where the limiting values for these neutral curves as $kh \to 0$ and $kh \to \infty$ are computed from Eqs. (46), (48), (52), (54), (56) and (58) and given in Table 2.

**Example 1.** Both inner and outer layers are equi-biaxially deformed in $(x_1x_2)$-plane i.e., $\lambda_1 = \lambda_2 = \lambda$ and $\lambda_1^* = \lambda_2^* = \lambda^*$ and from Section 2 for any strain energy function $\bar{\alpha} = \bar{\beta} = \bar{\alpha}^* = \bar{\beta}^* = 1$. The other prescribed parameters are $r = 0.25$, $a = 1.25$, $\sigma = -1.0$ and $D = 1$. This example corresponds to Case 3 in Section 4.2.2 with a limiting squared phase speed of the composite $\xi_{CL} = \xi_{S1}^*/a = 0.8$.

The dispersion curves are shown in Fig. 2 and it is seen from Fig. 2(a)–(c) that the squared phase speed of the fundamental mode of anti-symmetric waves $\xi_A^{(1)}$ is not always positive because $\xi_0^{(A)} = -0.875$ in Table 1,

Table 1
Limits of non-dimensional squared phase speed $\xi$

| | $kh \to 0$ | | | | $kh \to \infty$ | | | | | | | |
|---|---|---|---|---|---|---|---|---|---|---|---|---|
| | $\xi_0^{(A)}$ | $\xi_{01}^{(A)}$ | $\xi_0^{(S)}$ | $\xi_{02}^{(S)}$ | $\xi_{S1}$ | $\xi_{S2}$ | $\xi_{S1}^*/a$ | $\xi_{S2}^*/a$ | $\xi_{CL}$ | $\xi_R$ | $\xi_{IP}$ | $\xi_{IS}$ |
| Example 1 | −0.875 | 6.0 | 4.0 | 3.6 | 1[a] | – | 0.8[b] | – | 0.8 | 0.568 | 0.782 | 0.663 |
| Example 2 | 0.743 | 5.0 | 1.892 | 1.406 | 1[a] | – | – | 1.25[b] | 1.0 | 0.771 | – | – |
| Example 3 | 1.255 | 5.441 | 1.144 | 0.606 | 2.411[a] | – | – | 0.813[b] | 0.813 | 2.354 | – | 0.803 |
| Example 4 | 1.674 | 7.7 | 7.85 | 8.0 | – | 4.4[a] | – | 5.0[b] | 4.4 | 3.937 | – | 4.157 |

$\xi_{02}^{(A)} = \xi_0^{(A)}$ and $\xi_{01}^{(S)} = \xi_{01}^{(A)}$.

[a] $\xi_L$.

[b] $\xi_L^*/a$.

Table 2
Limits of non-dimensional Cauchy stress $\sigma$ for neutral curves

| | $kh \to 0$ | | | | | $kh \to \infty$ | | | |
|---|---|---|---|---|---|---|---|---|---|
| | $\sigma_0^{-(\mathrm{A})}$ | $\sigma_0^{+(\mathrm{A})}$ | $\sigma_{01}^{(\mathrm{A})}$ | $\sigma_0^{(\mathrm{S})}$ | $\sigma_{02}^{(\mathrm{S})}$ | $\sigma_{\mathrm{R}}^{-}$ | $\sigma_{\mathrm{R}}^{+}$ | $\sigma_{\mathrm{IS}}^{-}$ | $\sigma_{\mathrm{IS}}^{+}$ |
| Example 1 | 0 | 3.2 | 2 | 5 | 8 | −2 | 2 | −4 | 4 |
| Example 2 | −1.236 | 3.236 | 2 | 3 | 4 | −2 | 2 | −4.577 | 3.113 |
| Example 3 | −1.314 | 2.456 | 2.721 | 2.573 | 2.425 | −3.766 | 2.641 | −4.874 | 2.500 |
| Example 4 | −1.176 | 3.176 | 3.1 | 3.175 | 3.25 | −5.3 | 3.1 | −5.523 | 3.176 |

$\sigma_{02}^{\pm(\mathrm{A})} = \sigma_0^{\pm(\mathrm{A})}$ and $\sigma_{01}^{(\mathrm{S})} = \sigma_{01}^{(\mathrm{A})}$.

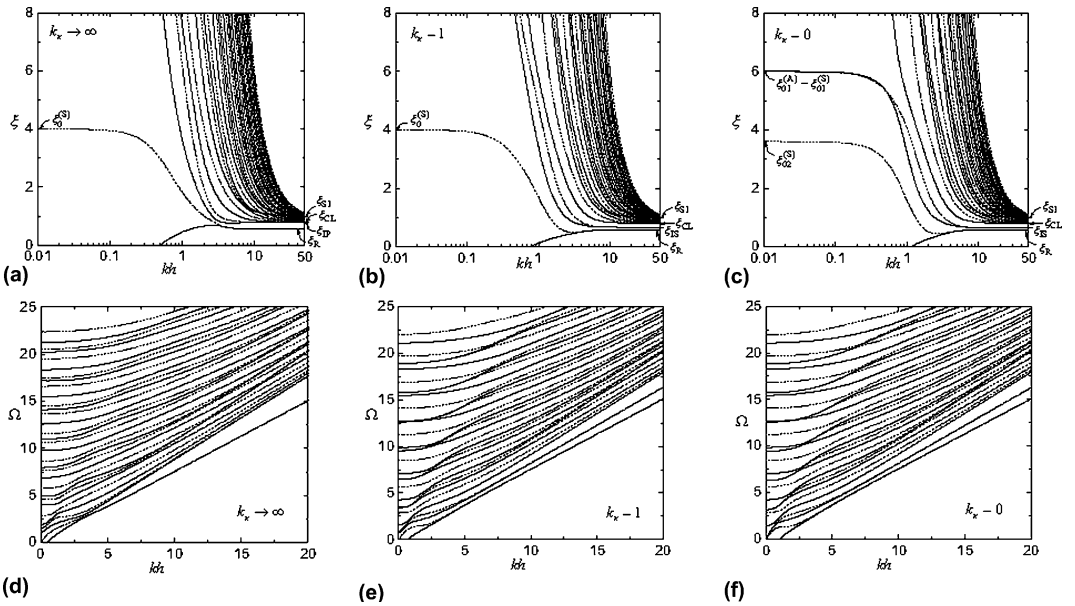


Fig. 2. Dispersion curves of the fundamental mode and next fifteen modes of Example 1. (a)–(c) Non-dimensional squared phase speed $\xi$, (d)–(f) non-dimensional frequency $\Omega$; solid lines for anti-symmetric waves and dashed lines for symmetric waves.

indicating that the fundamental mode is unstable for a certain range of $kh$. When $kh \to 0$ for $k_x > 0$, $\xi_{\mathrm{A}}^{(n)} \to \infty$ $(n = 2, 3, \ldots)$, while for the fully slipping case $\xi_{\mathrm{A}}^{(2)} \to \xi_{01}^{(\mathrm{A})}$ and $\xi_{\mathrm{A}}^{(n)} \to \infty$ $(n = 3, 4, \ldots)$. It is also seen from Fig. 2(c) that in the case of the fully slipping interface the squared phase speed of one mode of the anti-symmetric waves and one mode of the symmetric waves tend to the same limit i.e., $\xi_{01}^{(\mathrm{A})} = \xi_{01}^{(\mathrm{S})}$. When $kh \to \infty$ since, $\xi_{\mathrm{R}} < \xi_{\mathrm{IP}} < \xi_{\mathrm{CL}}$ and $\xi_{\mathrm{R}} < \xi_{\mathrm{IS}} < \xi_{\mathrm{CL}}$, for the perfectly bonded case $\xi_{\mathrm{A}}^{(1)} \to \xi_{\mathrm{R}}$, $\xi_{\mathrm{A}}^{(2)} \to \xi_{\mathrm{IP}}$ and $\xi_{\mathrm{A}}^{(n)} \to \xi_{\mathrm{CL}}$ $(n = 3, 4, \ldots)$ and for the imperfectly bonded and fully slipping interfaces cases $\xi_{\mathrm{A}}^{(1)} \to \xi_{\mathrm{R}}$, $\xi_{\mathrm{A}}^{(2)} \to \xi_{\mathrm{IS}}$ and $\xi_{\mathrm{A}}^{(n)} \to \xi_{\mathrm{CL}}$ $(n = 3, 4, \ldots)$. The frequency plots given in Fig. 2(d)–(f) show that when $kh \to 0$ for all values of $k_x$ the frequency of the fundamental mode $\Omega_{\mathrm{A}}^{(1)}$ has no real value, which corresponds to the negative limiting squared phase speed $\xi_0^{(\mathrm{A})} = -0.875$. The frequencies of the other modes tend to the cut-off frequencies calculated from Eq. (33), except when $k_x = 0$ (Fig. 2(f)), the frequency of the second mode $\Omega_{\mathrm{A}}^{(2)} \to 0$, which corresponds to the other finite limiting squared phase speed $\xi_{01}^{(\mathrm{A})} = 6.0$. From Fig. 2(f) it is seen that half of all of the modes of anti-symmetric waves have the same cut-off frequencies as symmetric waves since $\Omega_{\mathrm{C}}^{(\mathrm{A})} = n\pi, (n - \frac{1}{2})\pi/(\sqrt{a}D)$ and $\Omega_{\mathrm{C}}^{(\mathrm{S})} = n\pi, n\pi/(\sqrt{a}D)$, $(n = 1, 2, \ldots)$.

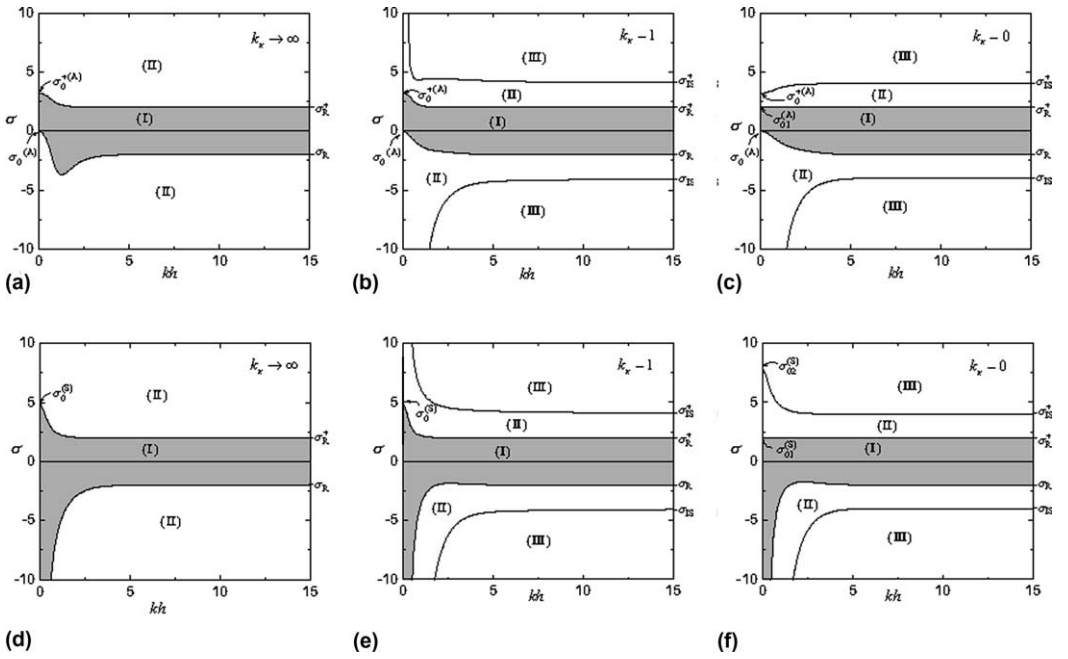


Fig. 3. Neutral curves corresponding to Example 1. (a)–(c) Anti-symmetric waves, (d)–(f) symmetric waves; shaded area is the region where all modes are stable.

The neutral curves for anti-symmetric and symmetric waves are shown in Fig. 3(a)–(c) and (d)–(f), respectively. Region (I) is the stable region (shaded area) where all modes have positive squared phase speeds. In region (II) only the fundamental mode has a squared phase speed which is negative, while both the fundamental mode and the next lowest mode have negative squared phase speeds in region (III). The limiting values of $\sigma$ are given in Table 2. When $kh \to 0$, in the case of anti-symmetric waves, the finite stable range for perfect and imperfect interfaces is $\sigma_0^{-(\mathrm{A})} < \sigma < \sigma_0^{+(\mathrm{A})}$ and for a fully slipping interface is $\sigma_{02}^{-(\mathrm{A})} (= \sigma_0^{-(\mathrm{A})}) < \sigma < \sigma_{01}^{(\mathrm{A})}$; while for symmetric waves, the stable range for perfect and imperfect interfaces is $\sigma < \sigma_0^{(\mathrm{S})}$ and for a fully slipping interface is $\sigma < \sigma_{01}^{(\mathrm{S})}$. When $kh \to \infty$, both kinds of waves have the same stable range, since $\sigma_{\mathrm{IS}}^- < \sigma_{\mathrm{R}}^-$ and $\sigma_{\mathrm{R}}^+ < \sigma_{\mathrm{IS}}^+$, $\sigma_{\mathrm{R}}^- < \sigma < \sigma_{\mathrm{R}}^+$ for all $k_x$. For $k_x = 0$, 1 and $\infty$ the numerical results indicate that if $0 < \sigma < 2$ anti-symmetric wave propagation is stable, while symmetric wave propagation will be stable if $-1.738 < \sigma < 2$. In Example 1, the non-dimensional Cauchy stress $\sigma = -1.0$ and when $kh \to 0$, $\xi_0^{(\mathrm{S})}$ is finite while $\xi_0^{(\mathrm{A})}$ does not exist. This behavior will also be reflected in the neutral curves (see Fig. 3) where when $\sigma = -1.0$ for anti-symmetric waves, region (I) does not exist for $0 < kh < kh_0$ where $kh_0$ depends on $k_x$ and $0.48 < kh_0 < 1.14$ while for symmetric waves, region (I) exists for all $kh$.

**Example 2.** The outer layers are equi-biaxially deformed in $(x_1x_2)$-plane i.e., $\bar{\alpha} = \bar{\beta} = 1$ and the inner layer is Varga material in a state of plane strain i.e., $\lambda_3^* = 1$ and $\lambda_1^* = \lambda_2^{*-1} = \lambda^*$ which yields $\bar{\alpha}^* = \lambda^{*4}$ and $\bar{\beta}^* = \lambda^{*2}$. Here $\lambda^*$ is prescribed as $\lambda^* = \sqrt{3}$ which yields $\bar{\alpha}^* = 9$ and $\bar{\beta}^* = 3$ and the other prescribed parameters are $r = 1$, $a = 6.4$, $\sigma = -0.5$ and $D = 1$. This example corresponds to Case 1 in Section 4.2.2 with a limiting squared phase speed $\xi_{\mathrm{CL}} = \xi_{\mathrm{S1}} = 1.0$.

The dispersion curves are shown in Fig. 4. From Fig. 4(a)–(c) it is seen that when $kh \to 0$, for $k_x > 0$, $\xi_{\mathrm{A}}^{(1)} \to \xi_0^{(\mathrm{A})}$ and $\xi_{\mathrm{A}}^{(n)} \to \infty$ $(n = 2, 3, \ldots)$, while for the fully slipping case $\xi_{\mathrm{A}}^{(1)} \to \xi_{02}^{(\mathrm{A})}$, $\xi_{\mathrm{A}}^{(2)} \to \xi_{01}^{(\mathrm{A})}$ and $\xi_{\mathrm{A}}^{(n)} \to \infty$ $(n = 3, 4, \ldots)$. When $kh \to \infty$, since there are no real values of $\xi_{\mathrm{IP}}$ and $\xi_{\mathrm{IS}}$, and $\xi_{\mathrm{R}} < \xi_{\mathrm{CL}}$ (see

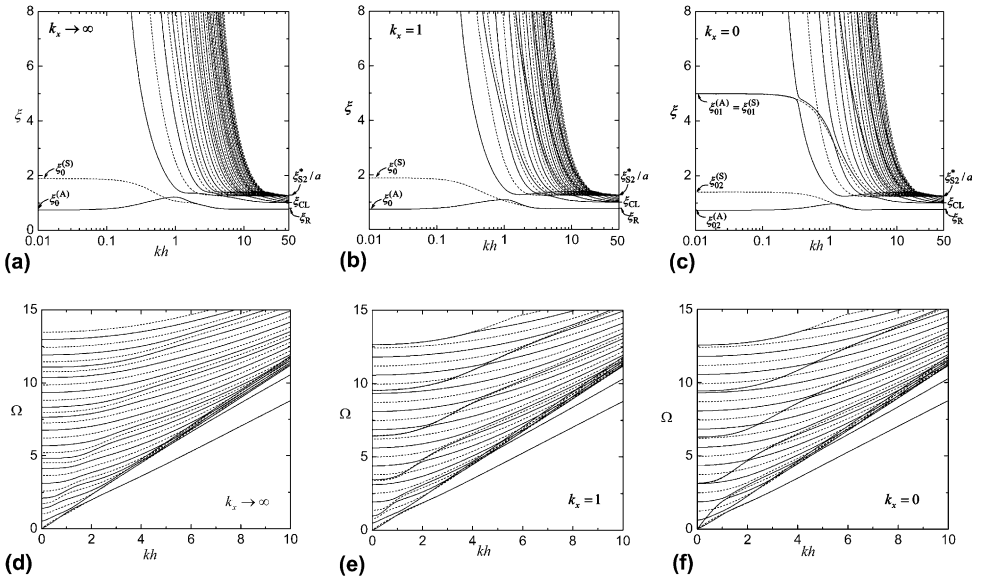


Fig. 4. Dispersion curves of the fundamental mode and next fifteen modes of Example 2. (a)–(c) Non-dimensional squared phase speed $\xi$, (d)–(f) non-dimensional frequency $\Omega$; solid lines for anti-symmetric waves and dashed lines for symmetric waves.

Table 1); $\xi_{\mathrm{A}}^{(1)} \to \xi_{\mathrm{R}}$ and $\xi_{\mathrm{A}}^{(n)} \to \xi_{\mathrm{CL}}$ $(n = 2, 3, \ldots)$ for all values of $k_x$. The frequency plots in Fig. 4(d)–(f) show that when $kh \to 0$ the frequencies of all modes tend to the cut-off frequencies calculated from Eq. (33), except in Fig. 4(d) and (e) for $k_x > 0$ where $\Omega_{\mathrm{A}}^{(1)} \to 0$ corresponding to the limiting squared phase speed $\xi_0^{(\mathrm{A})} = 0.743$; and in Fig. 4(f) for $k_x = 0$ where $\Omega_{\mathrm{A}}^{(1)} \to 0$ and $\Omega_{\mathrm{A}}^{(2)} \to 0$ corresponding to the two limiting squared phase speeds $\xi_{02}^{(\mathrm{A})} = 0.743$ and $\xi_{01}^{(\mathrm{A})} = 5.0$, respectively.

Fig. 5, shows the neutral curves where region (I) in Fig. 5(a)–(c) and Fig. 5(d)–(f) is the stable region for anti-symmetric waves and symmetric waves, respectively. For $k_x = 0$, 1 and $\infty$ the numerical results indicate that if $-1.236 < \sigma < 2$ anti-symmetric wave propagation is stable while if $-1.796 < \sigma < 2$ symmetric wave propagation will be stable. In this example since the non-dimensional Cauchy stress $\sigma = -0.5$ both types of waves are stable.

**Example 3.** The primary deformations of both inner and outer layers are plane strain deformations in $(x_1x_2)$-plane i.e., $\lambda_3 = 1$, $\lambda_1 = \lambda_2^{-1} = \lambda$, $\lambda_3^* = 1$ and $\lambda_1^* = \lambda_2^{*-1} = \lambda^*$. The outer and inner layers are Mooney–Rivlin and Varga materials, respectively, which yield $\bar{\alpha} = \lambda^4$, $2\bar{\beta} = \lambda^4 + 1$, $\bar{\alpha}^* = \lambda^{*4}$ and $\bar{\beta}^* = \lambda^{*2}$. Here $\lambda$ and $\lambda^*$ are prescribed as $\lambda = 1.25$ and $\lambda^* = 2.25$ which will give $\bar{\alpha} = 2.441$, $\bar{\beta} = 1.721$, $\bar{\alpha}^* = 25.629$ and $\bar{\beta}^* = 5.063$ and the other prescribed parameters are $r = 2.5$, $a = 20$, $\sigma = 0$ and $D = 1$. This example corresponds to Case 4 in Section 4.2.2 with a limiting squared phase speed of the composite $\xi_{\mathrm{CL}} = \xi_{\mathrm{S2}}^*/a = 0.813$.

From Fig. 6(a)–(c) it is seen that when $kh \to 0$, the behavior is similar to Example 2. The limiting values in Table 1 show that there is no real value of $\xi_{\mathrm{IP}}$ and $\xi_{\mathrm{IS}} < \xi_{\mathrm{CL}} < \xi_{\mathrm{R}}$; therefore, when $kh \to \infty$, for the perfectly bonded case $\xi_{\mathrm{A}}^{(n)} \to \xi_{\mathrm{CL}}$ $(n = 1, 2, \ldots)$, while for the imperfectly bonded and the fully slipping interface cases $\xi_{\mathrm{A}}^{(1)} \to \xi_{\mathrm{IS}}$ and $\xi_{\mathrm{A}}^{(n)} \to \xi_{\mathrm{CL}}$ $(n = 2, 3, \ldots)$. However, since $\xi_{\mathrm{IS}} = 0.803$ and $\xi_{\mathrm{CL}} = 0.813$ are very close together, separation of the limits of fundamental mode and the next higher modes are not clearly seen in Fig. 6(b) and (c). The frequency plots in Fig. 6(d)–(f) show that the behavior is similar to Example 2 when $kh \to 0$ and the frequencies of all modes tend to the cut-off frequencies calculated from Eq. (33), except the modes which correspond to the finite limiting phase speeds as $kh \to 0$.

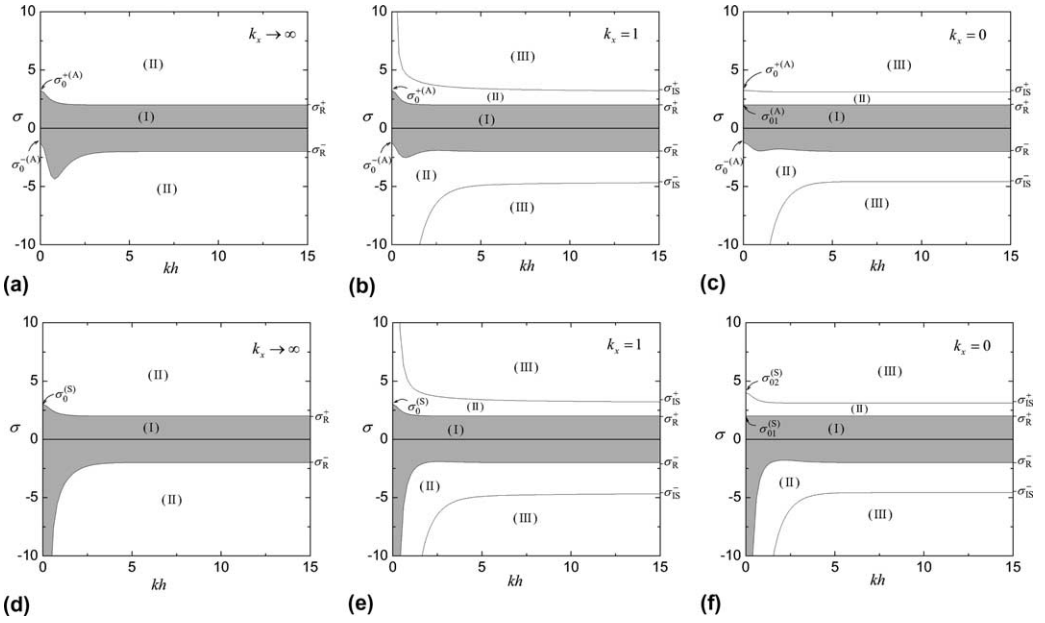


Fig. 5. Neutral curves corresponding to Example 2. (a)–(c) Anti-symmetric waves, (d)–(f) symmetric waves; shaded area is the region where all modes are stable.

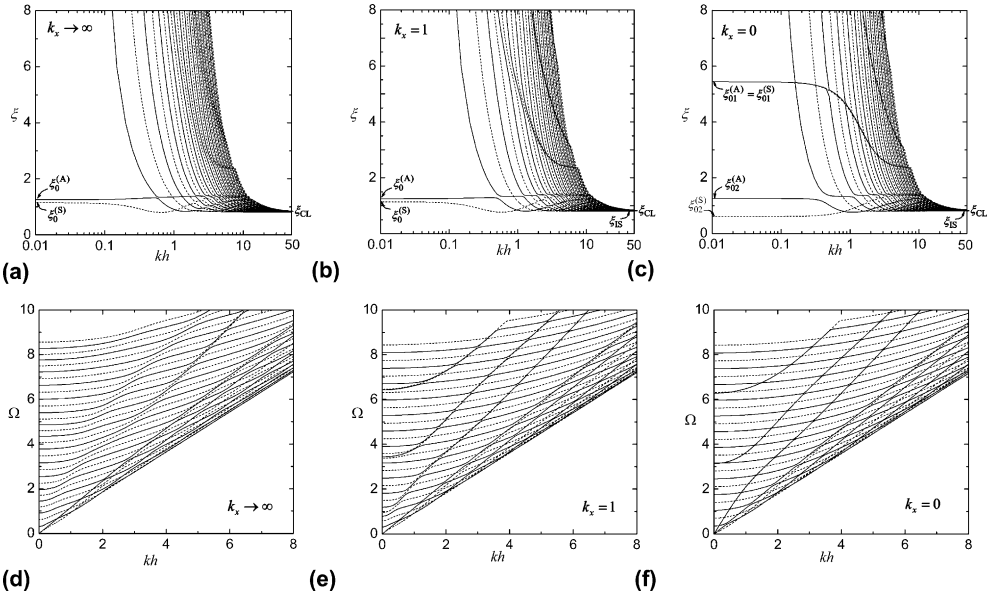


Fig. 6. Dispersion curves of the fundamental mode and next fifteen modes of Example 3. (a)–(c) Non-dimensional squared phase speed $\xi$, (d)–(f) non-dimensional frequency $\Omega$; solid lines for anti-symmetric waves and dashed lines for symmetric waves.

The neutral curves and stable regions are shown in Fig. 7 and the limiting values of $\sigma$ are shown in Table 2. In this example, since $\sigma_0^{+(A)} < \sigma_{01}^{(A)}$, in the case of anti-symmetric waves, the finite stable range when

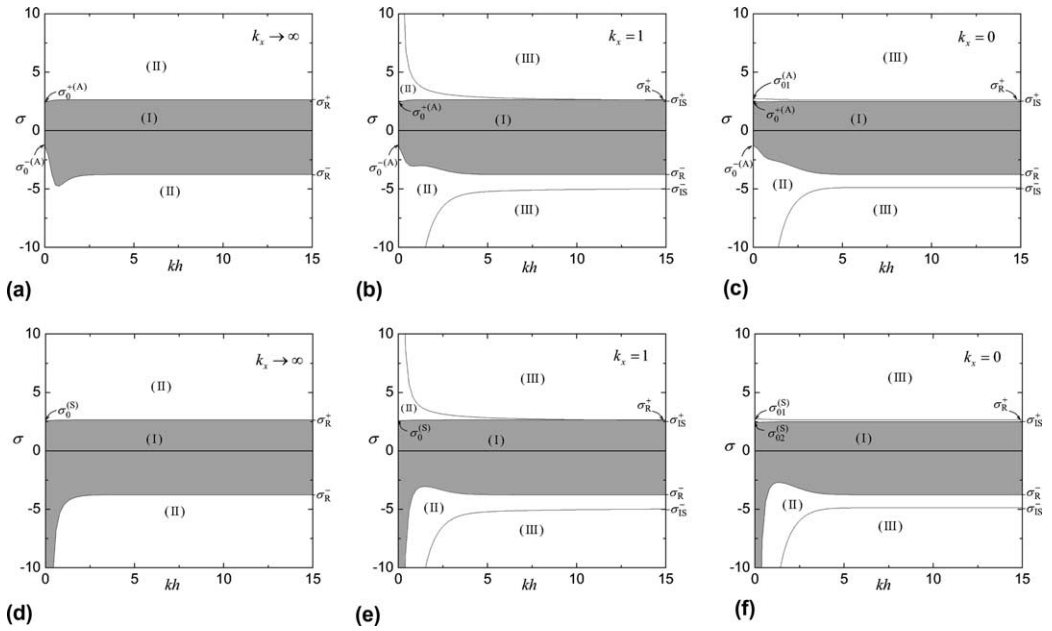


Fig. 7. Neutral curves corresponding to Example 3. (a)–(c) Anti-symmetric waves, (d)–(f) symmetric waves; shaded area is the region where all modes are stable.

$kh \to 0$ for all values of $k_x$ is $\sigma_0^{-(\mathrm{A})} < \sigma < \sigma_0^{+(\mathrm{A})}$; while for symmetric waves, the stable range for perfect and imperfect interface conditions is $\sigma < \sigma_0^{(\mathrm{S})}$ and for the fully slipping interface is $\sigma < \sigma_{02}^{(\mathrm{S})}$. When $kh \to \infty$, both kind of waves have the same stable range. Since $\sigma_{\mathrm{IS}}^- < \sigma_{\mathrm{R}}^-$ and $\sigma_{\mathrm{IS}}^+ < \sigma_{\mathrm{R}}^+$, the stable range is $\sigma_{\mathrm{R}}^- < \sigma < \sigma_{\mathrm{R}}^+$ for perfectly bonded case, and $\sigma_{\mathrm{R}}^- < \sigma < \sigma_{\mathrm{IS}}^+$ for imperfectly bonded and fully slipping interface cases. For $k_x = 0$, 1 and $\infty$ the numerical results indicate that if $-1.314 < \sigma < 2.456$ anti-symmetric wave propagation is stable, while if $-2.705 < \sigma < 2.425$ symmetric wave propagation will be stable. Since, $\sigma = 0$, in Example 3 both anti-symmetric and symmetric waves will be stable. In the imperfectly bonded and fully slipping interface cases when $\sigma > 0$ and when $kh$ increases, it is seen that region (II) decreases rapidly.

**Example 4.** Both inner and outer layers are Varga materials, the outer layers are pre-stressed by uniaxial tension in $x_1$-direction i.e., $\lambda_1 = \lambda$ and $\lambda_2 = \lambda_3 = \lambda^{-1/2}$ while the inner layer is in a state of plane strain in $(x_1x_2)$-plane i.e., $\lambda_3^* = 1$ and $\lambda_1^* = \lambda_2^{*-1} = \lambda^*$ which yield $\bar{\alpha} = \lambda^3$, $\bar{\beta} = \lambda^{3/2}$, $\bar{\alpha}^* = \lambda^{*4}$ and $\bar{\beta}^* = \lambda^{*2}$. Here $\lambda$ and $\lambda^*$ are prescribed as $\lambda = \sqrt[3]{4.41}$ and $\lambda^* = 1.5$ which results in $\bar{\alpha} = 4.41$, $\bar{\beta} = 2.1$, $\bar{\alpha}^* = 5.063$ and $\bar{\beta}^* = 2.25$ and the other prescribed parameters are $r = 1$, $a = 1$, $\sigma = -0.75$ and $D = 1$. This example corresponds to Case 2 in Section 4.2.2 with a limiting squared phase speed of the composite $\xi_{\mathrm{CL}} = \xi_{\mathrm{S2}} = 4.4$.

From Fig. 8(a)–(c) it can be seen that when $kh \to 0$, the behavior is similar to Examples 2 and 3. Since there is no real value for $\xi_{\mathrm{IP}}$ and $\xi_{\mathrm{R}} < \xi_{\mathrm{IS}} < \xi_{\mathrm{CL}}$, when $kh \to \infty$, for the perfectly bonded case $\xi_{\mathrm{A}}^{(1)} \to \xi_{\mathrm{R}}$ and $\xi_{\mathrm{A}}^{(n)} \to \xi_{\mathrm{CL}}$ $(n = 2, 3, \ldots)$, while for the imperfectly bonded and the fully slipping interface cases $\xi_{\mathrm{A}}^{(1)} \to \xi_{\mathrm{R}}$, $\xi_{\mathrm{A}}^{(2)} \to \xi_{\mathrm{IS}}$ and $\xi_{\mathrm{A}}^{(n)} \to \xi_{\mathrm{CL}}$ $(n = 3, 4, \ldots)$. The frequency plots in Fig. 8(d)–(f) show that when $kh \to 0$ the frequencies of all anti-symmetric modes tend to the cut-off frequencies calculated from Eq. (33), except the modes which correspond to the finite limiting phase speeds as $kh \to 0$. In addition, since in this example $\sqrt{a}D = 1$, the cut-off frequencies for $k_x = 0$ are for anti-symmetric waves $n\pi/2$ $(n = 1, 2, \ldots)$ and for symmetric waves $n\pi$ $(n = 1, 2, \ldots)$ where pairs of symmetric modes will have the same cut-off frequency.

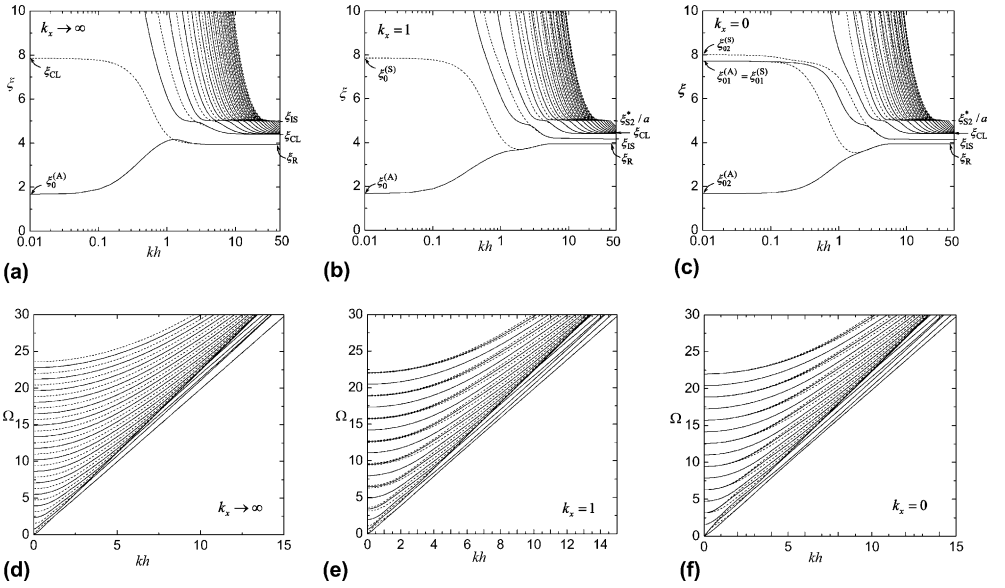


Fig. 8. Dispersion curves of the fundamental mode and next fifteen modes of Example 4. (a)–(c) Non-dimensional squared phase speed $\xi$, (d)–(f) non-dimensional frequency $\Omega$; solid lines for anti-symmetric waves and dashed lines for symmetric waves.

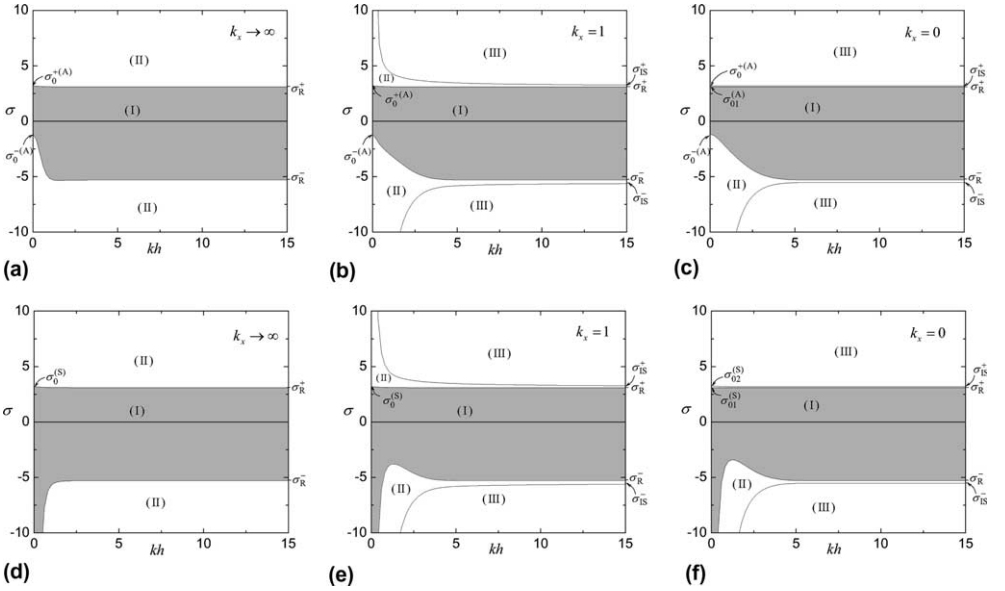


Fig. 9. Neutral curves corresponding to Example 4. (a)–(c) Anti-symmetric waves, (d)–(f) symmetric waves; shaded area is the region where all modes are stable.

The neutral curves and the stable regions are shown in Fig. 9. In the case of anti-symmetric waves, the stable range when $kh \to 0$ for perfect and imperfect interface is $\sigma_0^{-(A)} < \sigma < \sigma_0^{+(A)}$ and for fully slipping

interface is $\sigma_{02}^{-(A)}(=\sigma_0^{-(A)}) < \sigma < \sigma_{01}^{(A)}$; while for symmetric waves, the stable range for perfect and imperfect interface conditions is $\sigma < \sigma_0^{(S)}$ and for fully slipping interface is $\sigma < \sigma_{01}^{(S)}$. When $kh \to \infty$, both kind of waves have the same stable range $\sigma_R^- < \sigma < \sigma_R^+$ for all values of $k_x$. In addition, for $k_x = 0$, 1 and $\infty$ the numerical results indicate that if $-1.176 < \sigma < 3.1$ anti-symmetric wave propagation is stable, while symmetric wave propagation will be stable if $-3.414 < \sigma < 3.1$. In this example since $\sigma = -0.75$ both types of waves are stable. For the imperfectly bonded and the fully slipping interface cases for both tensile and compressive Cauchy stress $\sigma$, when $kh$ increases region (II) decreases rapidly.

## 7. Summary and conclusions

In the present analysis, the dispersive behavior of in-plane time harmonic anti-symmetric waves in a pre-stressed incompressible symmetric layered composite with imperfectly bonded interfaces is studied. The dispersion relation obtained for anti-symmetric waves differs from the corresponding case for symmetric waves, through the elements of the propagator matrix associated with the inner layer. The limiting squared phase speeds at both low and high wavenumber limits, the cut-off frequencies and stability considerations are discussed in detail.

The behavior of the dispersion curves for anti-symmetric waves is for the most part similar to that of symmetric waves at the low and high wavenumber limits. At low wavenumber limit, depending on the pre-stress for perfectly bonded and imperfectly bonded interfaces at most only one finite limiting squared phase speed may exist, while for the fully slipping interface case at most two finite limiting squared phase speeds may exist. For higher modes which have infinite squared phase speeds when $kh \to 0$, the equation to obtain the cut-off frequencies is derived. At high wavenumber limit as $kh \to \infty$, both anti-symmetric and symmetric waves tend to the same limiting squared phase speeds.

For both anti-symmetric and symmetric waves, the bifurcation equations obtained for imperfect interface and fully slipping interface cases are in the form of quartic equations of $\sigma$, while for the perfectly bonded case quadratic equations are obtained. Hence, in general for layered composites with imperfect or fully slipping interfaces there are four branches of neutral curves, while for the perfectly bonded case there are only two branches. The stable region is the area between the inner branches, because if $\sigma$ is outside this region the fundamental mode will have a negative squared phase speed, while when $\sigma$ is beyond the outer branches two negative squared phase speeds will be obtained for the fundamental and the next lowest modes. The stable ranges of $\sigma$ at the low wavenumber limit for the imperfect interface case are the same as for the perfectly bonded case, while at the high wavenumber limit the stable ranges of imperfect bonded case are the same as for the fully slipping interface case. For all $k_x$, symmetric wave propagation is stable in the low wavenumber region even if the composite is pre-stressed by large compression, while anti-symmetric waves will not be stable in the low wavenumber region if the composite is pre-stressed beyond the finite stable range.

## Acknowledgements

The first author gratefully acknowledges a Monbukagakusho scholarship from the Japanese government for doctoral students. The original title of this paper was "Flexural waves in pre-stressed imperfectly bonded incompressible elastic layered composites". The present title the authors feel is more appropriate for waves in pre-stressed layered structures as pre-stress precludes bending in the classical sense, and are grateful to an anonymous reviewer for this suggestion.

## Appendix A. The elements of propagator matrix

The elements of propagator matrix $\mathbf{P}(h)$ are given by

$$\begin{aligned}
P_{11} &= \gamma q_1 q_2 [f(q_2)C_2 - f(q_1)C_1]\kappa^{-1}, & P_{12} &= \gamma q_1 q_2 [q_1 f(q_2)S_1 - q_2 f(q_1)S_2]\kappa^{-1},\\
P_{13} &= q_1 q_2 [q_2 S_2 - q_1 S_1]\kappa^{-1}, & P_{14} &= q_1 q_2 [C_1 - C_2]\kappa^{-1},\\
P_{21} &= \gamma [q_1 f(q_2)S_2 - q_2 f(q_1)S_1]\kappa^{-1}, & P_{22} &= \gamma q_1 q_2 [f(q_2)C_1 - f(q_1)C_2]\kappa^{-1},\\
P_{23} &= -P_{14}, & P_{24} &= (q_2 S_1 - q_1 S_2)\kappa^{-1},\\
P_{31} &= \gamma^2 [q_1 f(q_2)^2 S_2 - q_2 f(q_1)^2 S_1]\kappa^{-1}, & P_{32} &= \gamma^2 q_1 q_2 f(q_1) f(q_2)[C_1 - C_2]\kappa^{-1},\\
P_{33} &= P_{11}, & P_{34} &= -P_{21},\\
P_{41} &= -P_{32}, & P_{42} &= \gamma^2 q_1 q_2 [q_1 f(q_2)^2 S_1 - q_2 f(q_1)^2 S_2]\kappa^{-1},\\
P_{43} &= \gamma q_1 q_2 [q_2 f(q_1)S_2 - q_1 f(q_2)S_1]\kappa^{-1}, & P_{44} &= P_{22},
\end{aligned} \tag{A.1}$$

where

$$\begin{aligned}
&f(q_m) = 1 + q_m^2 - \sigma, \quad C_m = \cosh(q_m kh), \quad S_m = \sinh(q_m kh), \quad (m = 1, 2),\\
&\sigma = \sigma_2/\gamma, \quad \kappa = q_1 q_2 \gamma (q_1^2 - q_2^2).
\end{aligned} \tag{A.2}$$

The elements of propagator matrix $\mathbf{P}^*(d)$ are obtained from Eq. (A.1) by interchanging $P_{ij} \leftrightarrow P_{ij}^*$, $q_m \leftrightarrow q_m^*$, $f(q_m) \leftrightarrow f^*(q_m^*)$, $C_m \leftrightarrow C_m^*$, $S_m \leftrightarrow S_m^*$, $\gamma \leftrightarrow \gamma^*$ and $\kappa \leftrightarrow \kappa^*$ where

$$\begin{aligned}
&f^*(q_m^*) = 1 + q_m^{*2} - r\sigma, \quad C_m^* = \cosh(q_m^* Dkh), \quad S_m = \sinh(q_m^* Dkh), \quad (m = 1, 2),\\
&r = \gamma/\gamma^*, \quad D = d/h.
\end{aligned} \tag{A.3}$$

## Appendix B. Roots $q_1$, $q_2$, $q_1^*$ and $q_2^*$

The roots $q_1$, $q_2$, $q_1^*$ and $q_2^*$ calculated from Eqs. (27) and (28) may be either real, complex or pure imaginary (Table 3).

Table 3
Roots $q_1$, $q_2$, $q_1^*$ and $q_2^*$

| | $\bar{\alpha} \leqslant 2\bar{\beta}$ | | | $\bar{\alpha} > 2\bar{\beta}$ | | | |
|---|---|---|---|---|---|---|---|
| | $0 < \xi < \xi_{S1}$[a] | $\xi = \xi_{S1}$ | $\xi_{S1} < \xi$ | $0 < \xi < \xi_{S2}$[a] | $\xi = \xi_{S2}$ | $\xi_{S2} < \xi \leqslant \xi_{S1}$ | $\xi_{S1} < \xi$ |
| $q_1$ | R or C | I | I | R or C | I | I | I |
| $q_2$ | R or C | R or C | R or C | R or C | I | I | R or C |
| | $\bar{\alpha}^* \leqslant 2\bar{\beta}^*$ | | | $\bar{\alpha}^* > 2\bar{\beta}^*$ | | | |
| | $0 < \xi^* < \xi_{S1}^*$[a] | $\xi^* = \xi_{S1}^*$ | $\xi_{S1}^* < \xi^*$ | $0 < \xi^* < \xi_{S2}^*$[a] | $\xi^* = \xi_{S2}^*$ | $\xi_{S2}^* < \xi^* \leqslant \xi_{S1}^*$ | $\xi_{S1}^* < \xi^*$ |
| $q_1^*$ | R or C | I | I | R or C | I | I | I |
| $q_2^*$ | R or C | R or C | R or C | R or C | I | I | R or C |

R—real, C—complex and I—pure imaginary.

[a] The strong ellipticity conditions Eq. (43) ensure that $\xi_{S1} > 0$ when $\bar{\alpha} \leqslant \bar{\beta}$; $\xi_{S2} > 0$ when $\bar{\alpha} > \bar{\beta}$; $\xi_{S1}^* > 0$ when $\bar{\alpha}^* \leqslant \bar{\beta}^*$; and $\xi_{S2}^* > 0$ when $\bar{\alpha}^* > \bar{\beta}^*$.

## References

Barnett, D.M., Gavazza, S.D., Lothe, J., 1988. Slip waves along the interface between two anisotropic elastic half-spaces in sliding contact. Proceedings of the Royal Society of London A 415, 389–419.

Dowaikh, M.A., Ogden, R.W., 1990. On surface waves and deformations in a pre-stressed incompressible elastic solid. IMA Journal of Applied Mathematics 44, 261–284.

Dowaikh, M.A., Ogden, R.W., 1991. Interfacial waves and deformations in pre-stressed elastic media. Proceedings of the Royal Society of London A 433, 313–328.

Gilbert, F., Backus, G.E., 1966. Propagator matrices in elastic wave and vibration problems. Geophysics 31, 326–332.

Kaplunov, J.D., Kossovich, L.Y., Nolde, E.V., 1998. Dynamics of Thin Walled Elastic Bodies. Academic Press, California.

Kaplunov, J.D., Nolde, E.V., Rogerson, G.A., 2000. A low-frequency model for dynamic motion in pre-stressed incompressible elastic structures. Proceedings of the Royal Society of London A 456, 2589–2610.

Kaplunov, J.D., Nolde, E.V., Rogerson, G.A., 2002. Short wave motion in a pre-stressed incompressible elastic plate. IMA Journal of Applied Mathematics 67, 383–399.

Kaplunov, J.D., Rogerson, G.A., 2002. An asymptotically consistent model for long-wave high-frequency motion in a pre-stressed elastic plate. Mathematics and Mechanics of Solids 7, 581–606.

Leungvichcharoen, S., Wijeyewickrema, A.C., 2003. Dispersion effects of extensional waves in pre-stressed imperfectly bonded incompressible elastic layered composites. Wave Motion 38, 311–325.

Nolde, E.V., Rogerson, G.A., 2002. Long wave asymptotic integration of the governing equations for a pre-stressed incompressible elastic layer with fixed faces. Wave Motion 36, 287–304.

Ogden, R.W., 1984. Non-linear Elastic Deformations. Ellis Harwood, Chichester.

Ogden, R.W., Roxburgh, D.G., 1993. The effect of pre-stress on the vibration and stability of elastic plates. International Journal of Engineering Science 31, 1611–1639.

Ogden, R.W., Sotiropoulos, D.A., 1995. On interfacial waves in pre-stressed layered incompressible elastic solids. Proceedings of the Royal Society of London A 450, 319–341.

Ogden, R.W., Sotiropoulos, D.A., 1997. The effect of pre-stress on the propagation and reflection of plane waves in incompressible elastic solids. IMA Journal of Applied Mathematics 59, 95–121.

Pichugin, A.V., Rogerson, G.A., 2001. A two-dimensional model for extensional motion of a pre-stressed incompressible elastic layer near cut-off frequencies. IMA Journal of Applied Mathematics 66, 357–385.

Rogerson, G.A., 1997. Some asymptotic expansions of the dispersion relation for an incompressible elastic plate. International Journal of Solids and Structures 34, 2785–2802.

Rogerson, G.A., Fu, Y., 1995. An asymptotic analysis of the dispersion relation of a pre-stressed incompressible elastic plate. Acta Mechanica 111, 59–74.

Rogerson, G.A., Sandiford, K.J., 1996. On small amplitude vibrations of pre-stressed laminates. International Journal of Engineering Science 34, 853–872.

Rogerson, G.A., Sandiford, K.J., 1997. Flexural waves in incompressible pre-stressed elastic composites. Quarterly Journal of Mechanics and Applied Mathematics 50, 597–624.

Rogerson, G.A., Sandiford, K.J., 1999. Harmonic wave propagation along a non-principal direction in a pre-stressed elastic plate. International Journal of Engineering Science 37, 1163–1691.

Rogerson, G.A., Sandiford, K.J., 2000. The effect of finite primary deformations on harmonic waves in layered elastic media. International Journal of Solids and Structures 37, 2059–2087.